Yellow to blue switching of fluorescence by the tuning of the pentaphenylphosphole structure: phosphorus electronic state vs. ring conjugation

Ruslan R. Shaydullin,[a] Alexey S. Galushko,[a] Evgeniy O. Pentsak,[a] Vladislav M. Korshunov,[b] Ilya V. Taydakov,[b] Evgeniy G. Gordeev,[a] Mikhail E. Minyaev,[a] Darina I. Nasyrova[a] and Valentine P. Ananikov[*a]

[a]Zelinsky Institute of Organic Chemistry, Russian Academy of Sciences, Moscow 119991, Russia

[b]Lebedev Physical Institute of the Russian Academy of Sciences, Moscow 119991, Russia

E-mail: val@ioc.ac.ru; https://AnanikovLab.ru

Synthesis of PPP, PPPO and H₂PPPO

Synthesis of PPP, PPPO and H$_2$PPPO

PPP was obtained according to previously described methods.[1,2].

The first steps in the synthesis of 1,2,3,4,5-pentaphenylphospholoxide (PPPO) and 1,2,3,4,5-pentaphenyl-2,5-dihydrophospholoxide (H$_2$PPPO) coincide with the synthesis of 1,2,3,4,5-pentaphenylphosphol (PPP).

Diphenylacetylene (2.67 g, 15 mmol) was dissolved in dry diethyl ether, and lithium (0.14 g, 20 mmol) was added to a Schlenk flask under argon. In this case, the dimerization of alkynes occurred with the appearance of a dark scarlet color of the solution. The reaction proceeded in an argon atmosphere for 5 hours. At the end of the reaction, the solution was filtered. Dichlorophenylphosphine (1.34 g, 7.5 mmol) in dry ether at 0 °C was added to the solution with organolithium compound (Scheme 1). The solution turned green, and lithium chloride precipitated out. The mixture was left for 24 hours after filtration, and the ether was removed under reduced pressure. The target product was obtained with a yield of 60%.
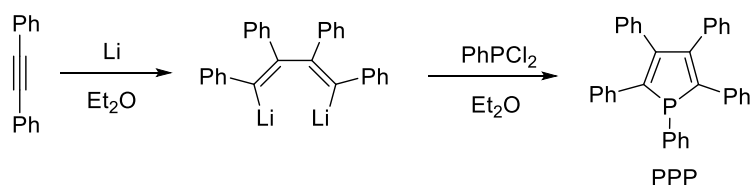
Scheme S1. Synthesis of PPP

To obtain PPPO and H$_2$PPPO, an additional stage of interaction of PPP with hydrogen peroxide in ethanol was carried out (Scheme 2). The dried reaction mixture of PPP was dissolved in 50 ml of ethanol, and then 0.935 ml of H$_2$O$_2$ was added dropwise, followed by stirring for 3 hours. The solvent was removed, and the resulting mixture was separated by gradient column chromatography.
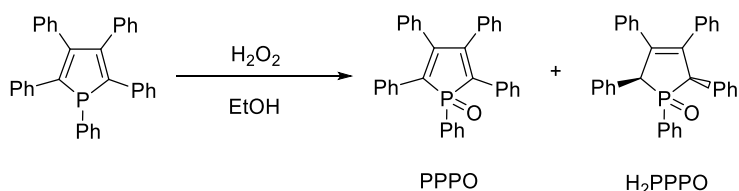
Scheme S2. Synthesis of PPPO and H$_2$PPPO.

The product mixture contained two fractions, one of which corresponded to PPPO and showed yellow fluorescence, and H$_2$PPPO, which showed intense blue fluorescence. After isolation, the PPPO yield was 40%, and the H$_2$PPPO yield was 12%.

NMR characterization

^{1}H and ^{13}C NMR spectra were obtained with a Bruker Fourier 300 HD NMR spectrometer (at frequencies of 300.1 and 75.5 MHz, respectively) in CDCl$_3$ solutions. Residual protons in CDCl$_3$ were used as internal standards. ^{31}P-NMR spectra were recorded on a Bruker DRX500 instrument (the frequencies for ^{31}P were 202.45 MHz) in CDCl$_3$. Eighty-five percent H$_3$PO$_4$ was used as a standard.

UV-vis and fluorescence spectra

UV-visible spectra at ambient temperature were recorded on a Varian Cary 5000 spectrophotometer. Luminescence and emission excitation spectra as well as the luminescence decays were recorded on a Fluorolog-QM-75-22-C spectrofluorometer equipped with a Hamamatsu R13456 cooled photomultiplier tube sensitive in the UV-Vis-NIR region (200-950 nm). All necessary instrument correction functions were applied for all spectra. Quantum yields were determined by the absolute method with the use of a G8 (GMP, Switzerland) integrating sphere placed into a Fluorolog QM spectrofluorometer. The measurements were conducted according to the procedure described previously.[3]
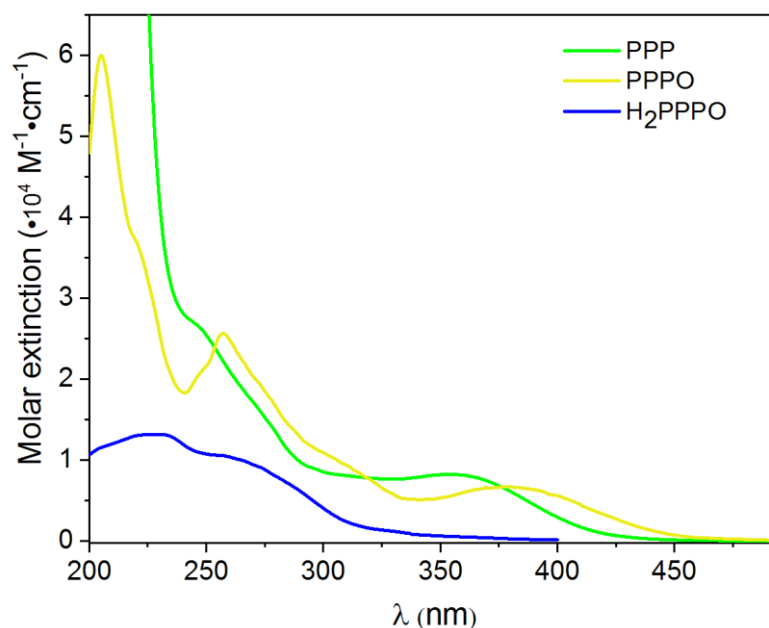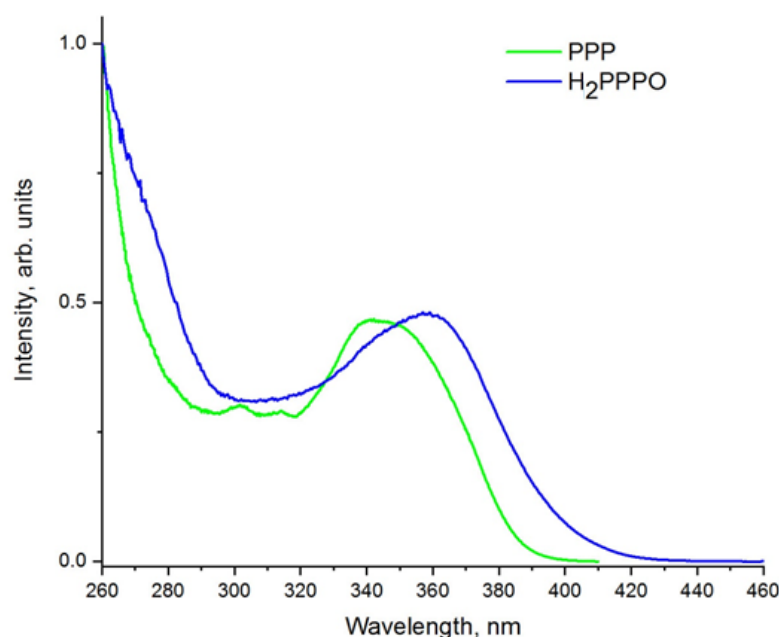

Figure S1. UV-Vis spectra.

Figure S2. Luminescence excitation spectra for H_2PPPO and PPP in solution MeCN.
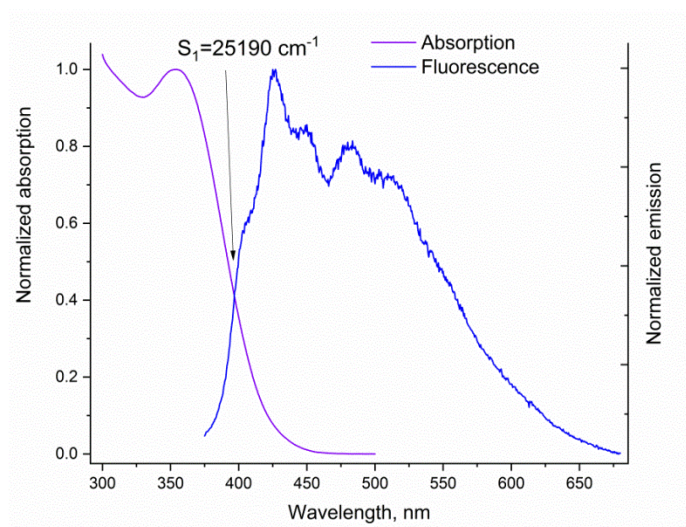
Figure S3. Normalized low-energy absorption band and normalized fluorescence spectra for H$_2$PPPO.
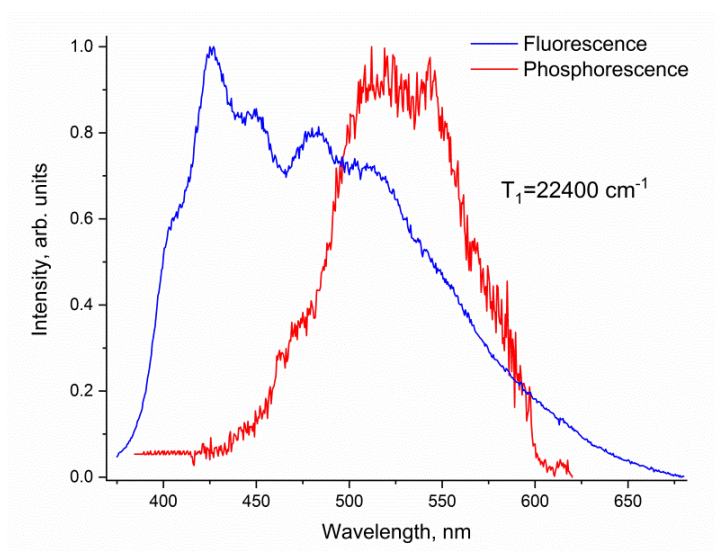

Figure S4. Fluorescence and phosphorescence spectra for H$_2$PPPO.
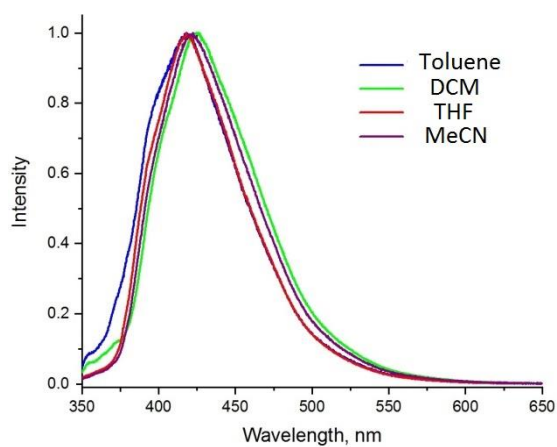

Figure S5. Luminescence spectra for H$_2$PPPO in different solutions.

ESI-MS

High-resolution ESI mass spectra were obtained with a Bruker maXis Q-TOF instrument. Measurements were carried out in positive ion mode (capillary voltage 4500 V, external calibration (electrospray calibration solution, Fluka)). The mass scan range was set to m/z 50—1500 Da. A syringe pump was used for the direct inlet of a solution of the analyte in acetonitrile (3 μL min^{-1}). Nitrogen was used as both the nebulizer gas (1.2 bar) and carrier gas (4.0 L min^{-1}, 200 °C). Experimental data were processed using Bruker DataAnalysis 4.0 software.
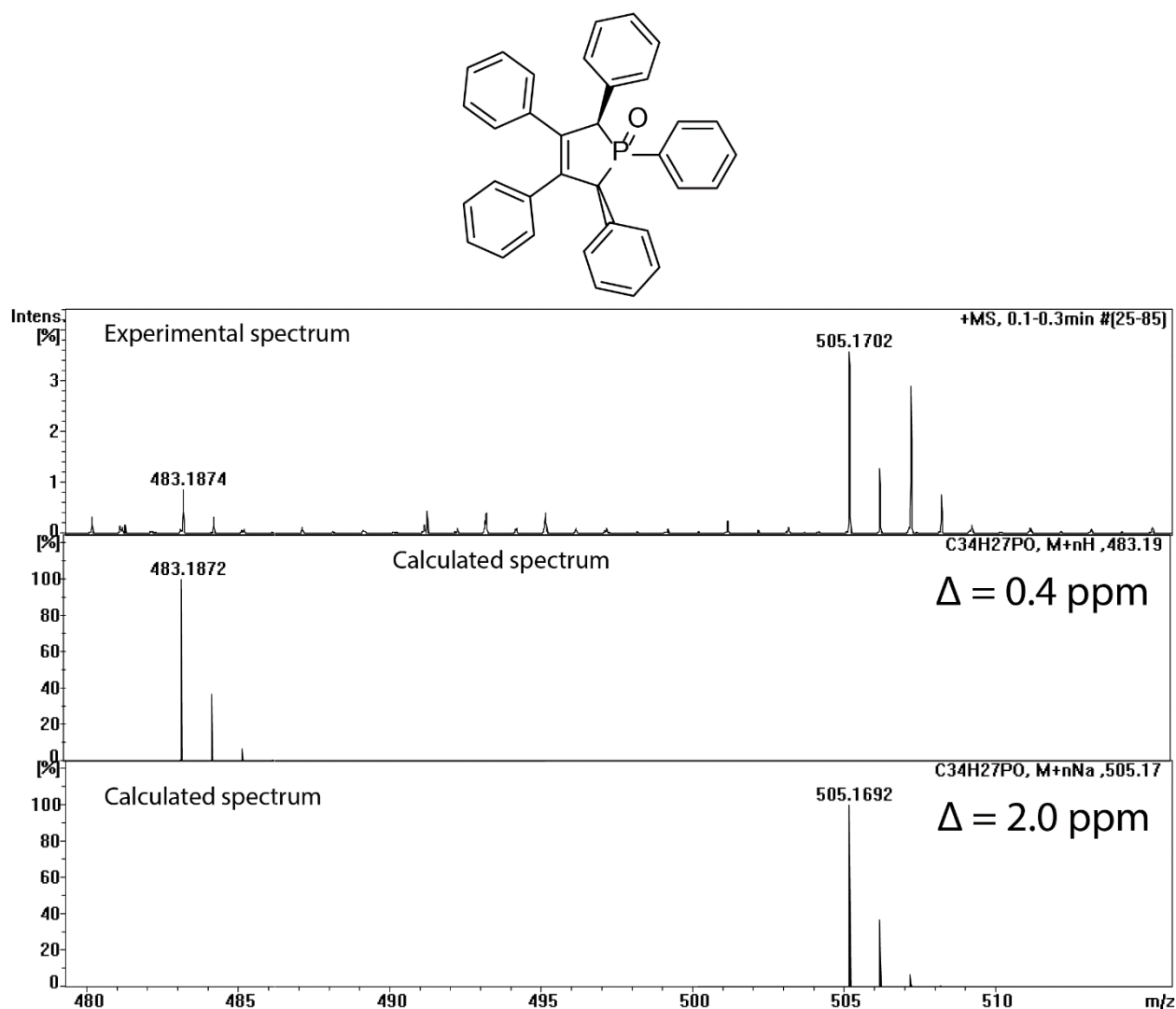
Figure S6. ESI-MS spectrum of H$_2$PPPO

X-ray crystallographic data and refinement details.

X-ray diffraction data were collected on a Bruker Quest D8 diffractometer equipped with a Photon-III area detector (shutterless φ- and ω-scan technique) using graphite-monochromatized Mo K$_\alpha$-radiation (λ=0.71073 Å). The intensity data were integrated by the SAINT program[4] and semiempirically corrected from equivalent reflections for absorption and decay with SADABS.[5]

The structures were solved by direct methods using SHELXT[6] and refined by the full-matrix least-squares on F^2 using SHELXL.[7] All nonhydrogen atoms were refined with anisotropic displacement parameters. All hydrogen atoms, including were placed in ideal calculated positions (C-H distance = 0.950 Å for aromatic, 0.990 Å for methylene and 1.000 Å for tertiary hydrogen atoms) and refined as riding atoms with relative isotropic displacement parameters. (1.2 U_{eq}(C) for hydrogen atoms). In PPPO, the U_{ij} components of anisotropic displacement parameters for atom C1 were restrained to approximate isotropic behavior. Crystal data, data collection and structure refinement details are summarized in Table S1.

Table S1. Crystal data, data collection and structure refinement details

Identification code	**PPPO**	**H$_2$PPPO**
Empirical formula	C$_{34}$H$_{25}$OP	C$_{34}$H$_{27}$OP
Formula weight	480.51	482.52
Temperature (K)	100(2)	100(2)
Crystal system	Monoclinic	Monoclinic
Space group	P2$_1$/c	P2$_1$/c
Unit cell dimensions		
a (Å)	16.0559(6)	11.6191(6)
b (Å)	6.2918(2)	5.9902(4)
c (Å)	24.2227(10)	35.856(2)
α (°)	90	90
β (°)	92.7170(10)	90.762(4)
γ (°)	90	90
Volume (Å^3)	2444.24(16)	2495.4(3)
Z	4	4
Calcd density (g/cm^3)	1.306	1.284
μ (mm^{-1})	0.139	0.136
F(000)	1008	1016
Crystal size (mm)	0.1×0.05×0.05	0.1×0.05×0.05
θ range (°)	2.060-30.033	2.076-26.500
Index ranges	-22<=h<=22,	-13<=h<=14,
	-8<=k<=8,	-7<=k<=7,
	-34<=l<=30	-45<=l<=45
Reflections		
collected	49922	45348
independent [R$_{int}$]	7133 [0.0544]	5191 [0.2032]
observed	5580	2721
Completeness to θ$_{max}$	0.998	1.000
T$_{max}$ / T$_{min}$	0.7468 / 0.7029	0.7461 / 0.6140

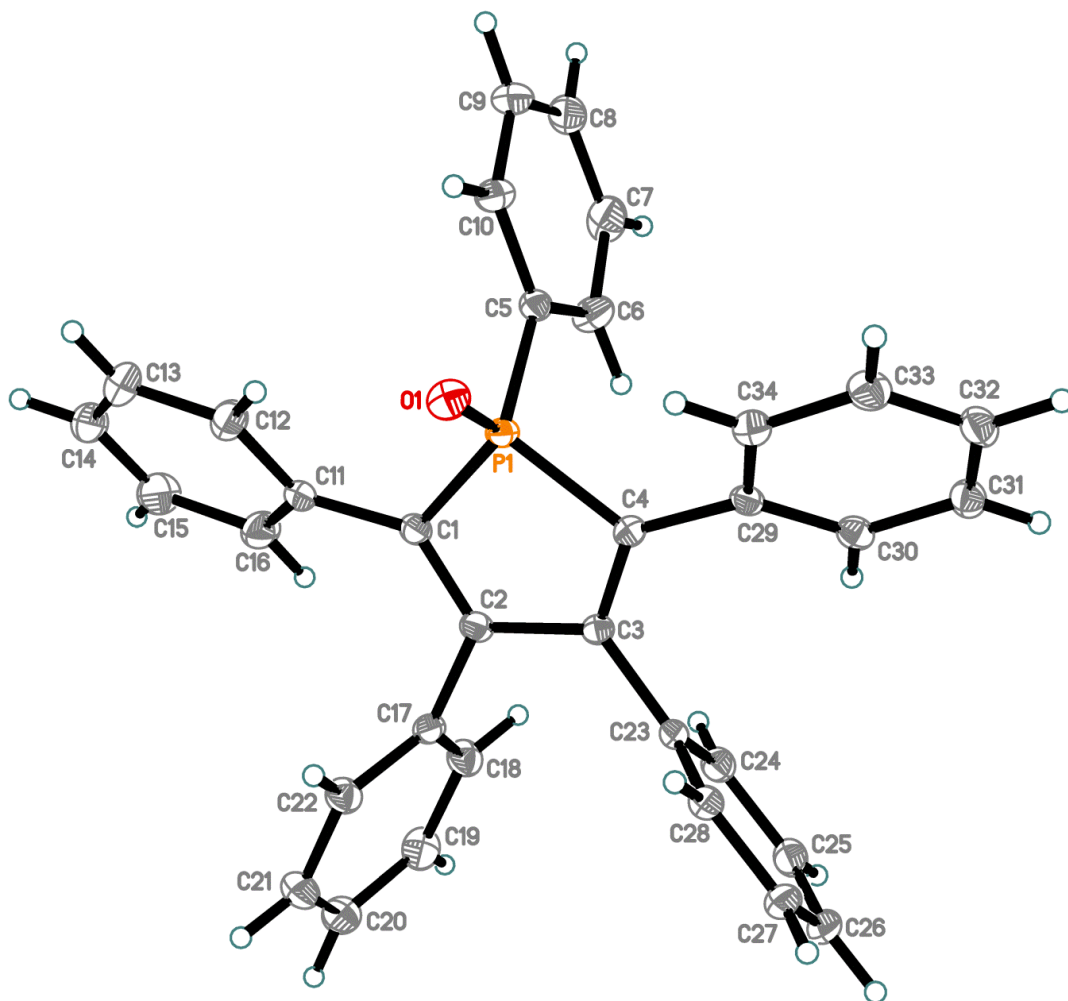|		
Restraints / parameters	7133 / 0 / 325	5191 / 6 / 325
Goodness-of-fit on F^2	1.096	1.041
R1 / wR2 [I>2σ(I)]	0.0543 / 0.1230	0.0879 / 0.1826
R1 / wR2 (all data)	0.0753 / 0.1378	0.1758 / 0.2302
$\Delta\rho_{max}$ / $\Delta\rho_{min}$ ($\bar{e}\cdot\text{Å}^{-3}$)	0.401 / -0.384	0.829 / -0.699
CCDC number	2095821	2095822

Figure S7. The molecular structure of **PPPO**. Thermal ellipsoids are set to a 50% probability level.

Table S2. Selected bond distances for **PPPO** (Å).

Atoms	Distance	Atoms	Distance	Atoms	Distance
P(1)-O(1)	1.4882(15)	C(5)-C(10)	1.399(3)	C(17)-C(22)	1.396(3)
P(1)-C(5)	1.7947(19)	C(6)-C(7)	1.389(3)	C(18)-C(19)	1.395(3)
P(1)-C(4)	1.8043(19)	C(7)-C(8)	1.387(3)	C(19)-C(20)	1.386(3)
P(1)-C(1)	1.8134(19)	C(8)-C(9)	1.380(3)	C(20)-C(21)	1.384(3)
C(1)-C(2)	1.354(3)	C(9)-C(10)	1.391(3)	C(21)-C(22)	1.393(3)
C(1)-C(11)	1.471(3)	C(11)-C(16)	1.398(3)	C(23)-C(28)	1.397(3)
C(2)-C(17)	1.493(3)	C(11)-C(12)	1.406(3)	C(23)-C(24)	1.398(3)
C(2)-C(3)	1.507(3)	C(12)-C(13)	1.390(3)	C(24)-C(25)	1.389(3)
C(3)-C(4)	1.358(3)	C(13)-C(14)	1.380(4)	C(25)-C(26)	1.386(3)
C(3)-C(23)	1.488(3)	C(14)-C(15)	1.388(4)	C(26)-C(27)	1.383(3)
C(4)-C(29)	1.476(3)	C(15)-C(16)	1.389(3)	C(27)-C(28)	1.391(3)
C(5)-C(6)	1.393(3)	C(17)-C(18)	1.395(3)	C(29)-C(34)	1.400(3)

Table S3. Selected bond angles for **PPPO** (°).

Atoms	Angle	Atoms	Angle
O(1)-P(1)-C(5)	111.53(9)	C(16)-C(11)-C(1)	122.59(19)
O(1)-P(1)-C(4)	117.12(9)	C(12)-C(11)-C(1)	119.28(18)
C(5)-P(1)-C(4)	109.29(9)	C(13)-C(12)-C(11)	120.8(2)
O(1)-P(1)-C(1)	115.77(9)	C(14)-C(13)-C(12)	120.3(2)
C(5)-P(1)-C(1)	108.14(9)	C(13)-C(14)-C(15)	119.5(2)
C(4)-P(1)-C(1)	93.48(9)	C(14)-C(15)-C(16)	120.6(2)
C(2)-C(1)-C(11)	130.08(17)	C(15)-C(16)-C(11)	120.6(2)
C(2)-C(1)-P(1)	108.67(14)	C(18)-C(17)-C(22)	118.77(18)
C(11)-C(1)-P(1)	121.24(14)	C(18)-C(17)-C(2)	122.49(18)
C(1)-C(2)-C(17)	124.58(17)	C(22)-C(17)-C(2)	118.74(18)
C(1)-C(2)-C(3)	114.34(16)	C(17)-C(18)-C(19)	120.3(2)
C(17)-C(2)-C(3)	120.68(16)	C(20)-C(19)-C(18)	120.3(2)
C(4)-C(3)-C(23)	122.96(17)	C(21)-C(20)-C(19)	119.67(19)
C(4)-C(3)-C(2)	114.80(16)	C(20)-C(21)-C(22)	120.2(2)
C(23)-C(3)-C(2)	121.98(16)	C(21)-C(22)-C(17)	120.6(2)
C(3)-C(4)-C(29)	129.40(17)	C(28)-C(23)-C(24)	119.21(18)
C(3)-C(4)-P(1)	108.53(14)	C(28)-C(23)-C(3)	118.58(17)
C(29)-C(4)-P(1)	122.05(14)	C(24)-C(23)-C(3)	122.15(18)
C(6)-C(5)-C(10)	120.10(18)	C(25)-C(24)-C(23)	119.73(19)
C(6)-C(5)-P(1)	122.74(15)	C(26)-C(25)-C(24)	120.78(19)
C(10)-C(5)-P(1)	117.12(15)	C(27)-C(26)-C(25)	119.78(19)
C(7)-C(6)-C(5)	119.4(2)	C(26)-C(27)-C(28)	120.06(19)
C(8)-C(7)-C(6)	120.3(2)	C(27)-C(28)-C(23)	120.44(19)
C(9)-C(8)-C(7)	120.6(2)	C(34)-C(29)-C(30)	118.73(17)
C(8)-C(9)-C(10)	119.7(2)	C(34)-C(29)-C(4)	118.99(17)
C(9)-C(10)-C(5)	119.8(2)	C(30)-C(29)-C(4)	122.22(17)
C(16)-C(11)-C(12)	118.07(19)	C(31)-C(30)-C(29)	120.18(18)

Table S4. Torsion angles for **PPPO** (°).

Atoms	Angle	Atoms	Angle
O(1)-P(1)-C(1)-C(2)	-118.58(14)	C(1)-C(11)-C(12)-C(13)	177.6(2)
C(5)-P(1)-C(1)-C(2)	115.47(15)	C(11)-C(12)-C(13)-C(14)	-0.3(4)
C(4)-P(1)-C(1)-C(2)	3.87(15)	C(12)-C(13)-C(14)-C(15)	-0.1(4)
O(1)-P(1)-C(1)-C(11)	60.16(18)	C(13)-C(14)-C(15)-C(16)	0.4(4)
C(5)-P(1)-C(1)-C(11)	-65.79(17)	C(14)-C(15)-C(16)-C(11)	-0.2(4)
C(4)-P(1)-C(1)-C(11)	-177.39(16)	C(12)-C(11)-C(16)-C(15)	-0.2(3)

C(11)-C(1)-C(2)-C(17)	-8.8(3)	C(1)-C(11)-C(16)-C(15)	-177.3(2)
P(1)-C(1)-C(2)-C(17)	169.78(15)	C(1)-C(2)-C(17)-C(18)	113.0(2)
C(11)-C(1)-C(2)-C(3)	178.44(19)	C(3)-C(2)-C(17)-C(18)	-74.7(2)
P(1)-C(1)-C(2)-C(3)	-3.0(2)	C(1)-C(2)-C(17)-C(22)	-66.5(3)
C(1)-C(2)-C(3)-C(4)	0.1(2)	C(3)-C(2)-C(17)-C(22)	105.8(2)
C(17)-C(2)-C(3)-C(4)	-172.93(17)	C(22)-C(17)-C(18)-C(19)	-1.2(3)
C(1)-C(2)-C(3)-C(23)	174.51(17)	C(2)-C(17)-C(18)-C(19)	179.28(19)
C(17)-C(2)-C(3)-C(23)	1.5(3)	C(17)-C(18)-C(19)-C(20)	-0.3(3)
C(23)-C(3)-C(4)-C(29)	7.3(3)	C(18)-C(19)-C(20)-C(21)	1.4(3)
C(2)-C(3)-C(4)-C(29)	-178.37(18)	C(19)-C(20)-C(21)-C(22)	-1.1(3)
C(23)-C(3)-C(4)-P(1)	-171.53(15)	C(20)-C(21)-C(22)-C(17)	-0.4(3)
C(2)-C(3)-C(4)-P(1)	2.8(2)	C(18)-C(17)-C(22)-C(21)	1.5(3)
O(1)-P(1)-C(4)-C(3)	117.59(14)	C(2)-C(17)-C(22)-C(21)	-178.95(18)
C(5)-P(1)-C(4)-C(3)	-114.38(14)	C(4)-C(3)-C(23)-C(28)	62.4(3)
C(1)-P(1)-C(4)-C(3)	-3.78(15)	C(2)-C(3)-C(23)-C(28)	-111.5(2)
O(1)-P(1)-C(4)-C(29)	-61.35(18)	C(4)-C(3)-C(23)-C(24)	-114.6(2)
C(5)-P(1)-C(4)-C(29)	66.69(17)	C(2)-C(3)-C(23)-C(24)	71.5(2)
C(1)-P(1)-C(4)-C(29)	177.28(16)	C(28)-C(23)-C(24)-C(25)	0.3(3)
O(1)-P(1)-C(5)-C(6)	172.42(16)	C(3)-C(23)-C(24)-C(25)	177.32(17)
C(4)-P(1)-C(5)-C(6)	41.33(19)	C(23)-C(24)-C(25)-C(26)	-0.2(3)
C(1)-P(1)-C(5)-C(6)	-59.18(19)	C(24)-C(25)-C(26)-C(27)	0.1(3)
O(1)-P(1)-C(5)-C(10)	-9.64(18)	C(25)-C(26)-C(27)-C(28)	-0.1(3)
C(4)-P(1)-C(5)-C(10)	-140.73(15)	C(26)-C(27)-C(28)-C(23)	0.2(3)
C(1)-P(1)-C(5)-C(10)	118.76(16)	C(24)-C(23)-C(28)-C(27)	-0.3(3)
C(10)-C(5)-C(6)-C(7)	-1.9(3)	C(3)-C(23)-C(28)-C(27)	-177.42(17)
P(1)-C(5)-C(6)-C(7)	175.94(17)	C(3)-C(4)-C(29)-C(34)	-145.9(2)
C(5)-C(6)-C(7)-C(8)	0.8(3)	P(1)-C(4)-C(29)-C(34)	32.8(2)
C(6)-C(7)-C(8)-C(9)	0.9(4)	C(3)-C(4)-C(29)-C(30)	36.9(3)
C(7)-C(8)-C(9)-C(10)	-1.5(3)	P(1)-C(4)-C(29)-C(30)	-144.42(16)
C(8)-C(9)-C(10)-C(5)	0.3(3)	C(34)-C(29)-C(30)-C(31)	0.9(3)
C(6)-C(5)-C(10)-C(9)	1.4(3)	C(4)-C(29)-C(30)-C(31)	178.12(17)
P(1)-C(5)-C(10)-C(9)	-176.61(16)	C(29)-C(30)-C(31)-C(32)	-1.1(3)
C(2)-C(1)-C(11)-C(16)	-32.6(3)	C(30)-C(31)-C(32)-C(33)	0.7(3)
P(1)-C(1)-C(11)-C(16)	148.95(17)	C(31)-C(32)-C(33)-C(34)	-0.2(3)
C(2)-C(1)-C(11)-C(12)	150.3(2)	C(32)-C(33)-C(34)-C(29)	0.1(3)
P(1)-C(1)-C(11)-C(12)	-28.1(3)	C(30)-C(29)-C(34)-C(33)	-0.4(3)
C(16)-C(11)-C(12)-C(13)	0.4(3)	C(4)-C(29)-C(34)-C(33)	-177.73(18)

Table S5. Atom deviations from the flat PC$_4$ cycle (atoms P1, C1..C4) in **PPPO** (Å).

Atom	P1	C1	C2	C3	C4
Deviation*	-0.0245(8)	0.0249(11)	-0.0129(12)	-0.0117(12)	0.0242(11)

* +/- signs state for deviations in different directions.

Table S6. Dihedral angle between the PC$_4$ and Ph planes in **PPPO** (°).

Phenyl	C11..C16	C17..C22	C23..C28	C29..C34
Deviation	30.633(83)	70.406(59)	65.859(65)	34.927(68)

The structure of H$_2$PPPO
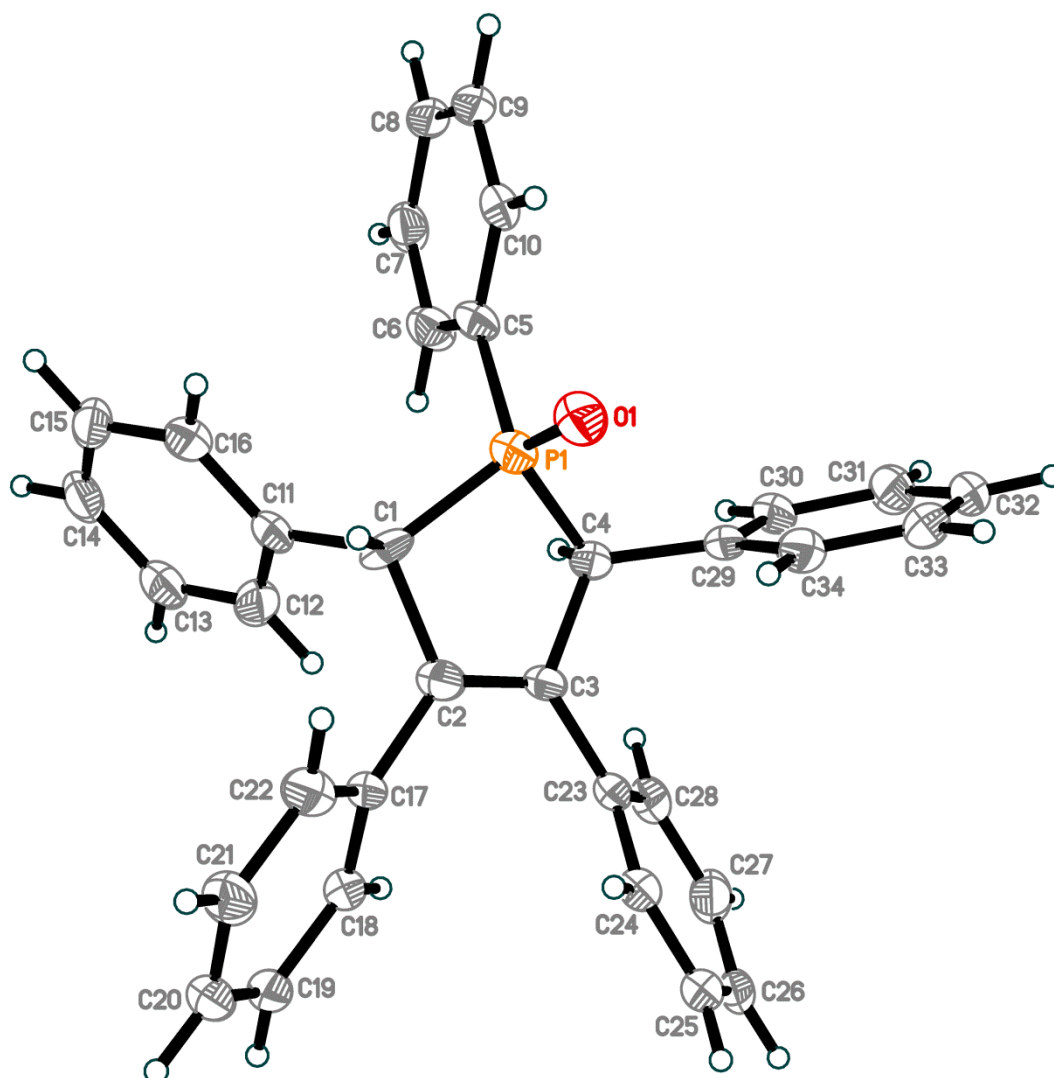
Figure S8. The molecular structure of **H$_2$PPPO**. Thermal ellipsoids are set to a 50% probability level.

Table S7. Selected bond distances for **H₂PPPO** (Å).

Atoms	Distance	Atoms	Distance	Atoms	Distance
P(1)-O(1)	1.489(4)	C(6)-C(7)	1.392(7)	C(19)-C(20)	1.376(8)
P(1)-C(1)	1.761(5)	C(7)-C(8)	1.376(7)	C(20)-C(21)	1.374(7)
P(1)-C(5)	1.795(5)	C(8)-C(9)	1.373(8)	C(21)-C(22)	1.400(7)
P(1)-C(4)	1.837(5)	C(9)-C(10)	1.384(7)	C(23)-C(28)	1.386(8)
C(1)-C(2)	1.544(6)	C(11)-C(12)	1.380(8)	C(23)-C(24)	1.394(7)
C(1)-C(11)	1.576(7)	C(11)-C(16)	1.394(7)	C(24)-C(25)	1.370(7)
C(2)-C(3)	1.346(7)	C(12)-C(13)	1.390(7)	C(25)-C(26)	1.383(9)
C(2)-C(17)	1.495(6)	C(13)-C(14)	1.385(8)	C(26)-C(27)	1.390(9)
C(3)-C(23)	1.479(7)	C(14)-C(15)	1.360(9)	C(27)-C(28)	1.390(7)
C(3)-C(4)	1.539(6)	C(15)-C(16)	1.402(8)	C(29)-C(30)	1.384(7)
C(4)-C(29)	1.516(6)	C(17)-C(18)	1.389(7)	C(29)-C(34)	1.390(7)
C(5)-C(6)	1.391(8)	C(17)-C(22)	1.393(8)	C(30)-C(31)	1.392(7)
C(5)-C(10)	1.396(7)	C(18)-C(19)	1.394(6)	C(31)-C(32)	1.390(8)

Table S8. Selected bond angles for **H₂PPPO** (°).

Atoms	Angle	Atoms	Angle
O(1)-P(1)-C(1)	109.2(2)	C(12)-C(11)-C(1)	122.2(5)
O(1)-P(1)-C(5)	112.3(2)	C(16)-C(11)-C(1)	119.1(5)
C(1)-P(1)-C(5)	114.2(2)	C(11)-C(12)-C(13)	121.3(5)
O(1)-P(1)-C(4)	115.6(2)	C(14)-C(13)-C(12)	119.3(6)
C(1)-P(1)-C(4)	95.5(2)	C(15)-C(14)-C(13)	120.5(6)
C(5)-P(1)-C(4)	109.0(3)	C(14)-C(15)-C(16)	120.4(5)
C(2)-C(1)-C(11)	110.4(4)	C(11)-C(16)-C(15)	119.9(6)
C(2)-C(1)-P(1)	103.5(3)	C(18)-C(17)-C(22)	118.3(4)
C(11)-C(1)-P(1)	117.4(3)	C(18)-C(17)-C(2)	122.1(5)
C(3)-C(2)-C(17)	126.9(5)	C(22)-C(17)-C(2)	119.5(5)
C(3)-C(2)-C(1)	114.9(4)	C(17)-C(18)-C(19)	120.6(5)
C(17)-C(2)-C(1)	118.1(4)	C(20)-C(19)-C(18)	120.4(5)
C(2)-C(3)-C(23)	126.2(4)	C(21)-C(20)-C(19)	120.0(5)
C(2)-C(3)-C(4)	115.8(4)	C(20)-C(21)-C(22)	119.8(5)
C(23)-C(3)-C(4)	118.0(4)	C(17)-C(22)-C(21)	120.8(5)
C(29)-C(4)-C(3)	117.1(4)	C(28)-C(23)-C(24)	118.0(5)
C(29)-C(4)-P(1)	113.2(4)	C(28)-C(23)-C(3)	120.0(5)
C(3)-C(4)-P(1)	101.1(3)	C(24)-C(23)-C(3)	122.0(5)
C(6)-C(5)-C(10)	119.7(5)	C(25)-C(24)-C(23)	121.8(6)
C(6)-C(5)-P(1)	124.6(4)	C(24)-C(25)-C(26)	119.8(6)

Atoms	Angle	Atoms	Angle
C(10)-C(5)-P(1)	115.6(4)	C(25)-C(26)-C(27)	119.9(5)
C(5)-C(6)-C(7)	119.5(5)	C(26)-C(27)-C(28)	119.6(6)
C(8)-C(7)-C(6)	120.8(5)	C(23)-C(28)-C(27)	121.0(6)
C(9)-C(8)-C(7)	119.4(5)	C(30)-C(29)-C(34)	118.7(4)
C(8)-C(9)-C(10)	121.3(5)	C(30)-C(29)-C(4)	120.2(5)
C(9)-C(10)-C(5)	119.3(6)	C(34)-C(29)-C(4)	121.0(5)
C(12)-C(11)-C(16)	118.7(5)	C(29)-C(30)-C(31)	121.3(5)

Table S9. Torsion angles for **H₂PPPO** (°).

Atoms	Angle	Atoms	Angle
O(1)-P(1)-C(1)-C(2)	-92.6(4)	C(1)-C(11)-C(12)-C(13)	-179.0(4)
C(5)-P(1)-C(1)-C(2)	140.7(3)	C(11)-C(12)-C(13)-C(14)	0.3(8)
C(4)-P(1)-C(1)-C(2)	26.9(4)	C(12)-C(13)-C(14)-C(15)	0.1(8)
O(1)-P(1)-C(1)-C(11)	145.5(4)	C(13)-C(14)-C(15)-C(16)	-0.5(8)
C(5)-P(1)-C(1)-C(11)	18.8(5)	C(12)-C(11)-C(16)-C(15)	0.1(7)
C(4)-P(1)-C(1)-C(11)	-94.9(4)	C(1)-C(11)-C(16)-C(15)	178.7(4)
C(11)-C(1)-C(2)-C(3)	107.0(5)	C(14)-C(15)-C(16)-C(11)	0.4(8)
P(1)-C(1)-C(2)-C(3)	-19.5(6)	C(3)-C(2)-C(17)-C(18)	-44.4(8)
C(11)-C(1)-C(2)-C(17)	-68.9(6)	C(1)-C(2)-C(17)-C(18)	130.8(5)
P(1)-C(1)-C(2)-C(17)	164.7(4)	C(3)-C(2)-C(17)-C(22)	139.3(6)
C(17)-C(2)-C(3)-C(23)	-3.6(9)	C(1)-C(2)-C(17)-C(22)	-45.4(7)
C(1)-C(2)-C(3)-C(23)	-179.0(5)	C(22)-C(17)-C(18)-C(19)	-0.8(7)
C(17)-C(2)-C(3)-C(4)	174.3(5)	C(2)-C(17)-C(18)-C(19)	-177.1(4)
C(1)-C(2)-C(3)-C(4)	-1.1(7)	C(17)-C(18)-C(19)-C(20)	0.3(7)
C(2)-C(3)-C(4)-C(29)	143.4(5)	C(18)-C(19)-C(20)-C(21)	-0.2(8)
C(23)-C(3)-C(4)-C(29)	-38.5(7)	C(19)-C(20)-C(21)-C(22)	0.6(8)
C(2)-C(3)-C(4)-P(1)	20.0(5)	C(18)-C(17)-C(22)-C(21)	1.2(8)
C(23)-C(3)-C(4)-P(1)	-161.9(4)	C(2)-C(17)-C(22)-C(21)	177.6(5)
O(1)-P(1)-C(4)-C(29)	-38.8(4)	C(20)-C(21)-C(22)-C(17)	-1.1(8)
C(1)-P(1)-C(4)-C(29)	-153.1(4)	C(2)-C(3)-C(23)-C(28)	135.1(6)
C(5)-P(1)-C(4)-C(29)	88.8(4)	C(4)-C(3)-C(23)-C(28)	-42.7(6)
O(1)-P(1)-C(4)-C(3)	87.3(3)	C(2)-C(3)-C(23)-C(24)	-45.3(8)
C(1)-P(1)-C(4)-C(3)	-27.1(4)	C(4)-C(3)-C(23)-C(24)	136.9(5)
C(5)-P(1)-C(4)-C(3)	-145.1(3)	C(28)-C(23)-C(24)-C(25)	-0.6(7)
O(1)-P(1)-C(5)-C(6)	173.4(4)	C(3)-C(23)-C(24)-C(25)	179.8(4)
C(1)-P(1)-C(5)-C(6)	-61.6(5)	C(23)-C(24)-C(25)-C(26)	0.4(8)
C(4)-P(1)-C(5)-C(6)	43.9(5)	C(24)-C(25)-C(26)-C(27)	-0.1(8)
O(1)-P(1)-C(5)-C(10)	-6.1(5)	C(25)-C(26)-C(27)-C(28)	0.1(8)

C(1)-P(1)-C(5)-C(10)	119.0(4)	C(24)-C(23)-C(28)-C(27)	0.5(7)
C(4)-P(1)-C(5)-C(10)	-135.6(4)	C(3)-C(23)-C(28)-C(27)	-179.9(4)
C(10)-C(5)-C(6)-C(7)	-0.7(7)	C(26)-C(27)-C(28)-C(23)	-0.3(7)
P(1)-C(5)-C(6)-C(7)	179.9(4)	C(3)-C(4)-C(29)-C(30)	124.7(5)
C(5)-C(6)-C(7)-C(8)	0.4(8)	P(1)-C(4)-C(29)-C(30)	-118.3(5)
C(6)-C(7)-C(8)-C(9)	-0.1(8)	C(3)-C(4)-C(29)-C(34)	-58.5(7)
C(7)-C(8)-C(9)-C(10)	0.1(7)	P(1)-C(4)-C(29)-C(34)	58.5(5)
C(8)-C(9)-C(10)-C(5)	-0.4(7)	C(34)-C(29)-C(30)-C(31)	-1.2(7)
C(6)-C(5)-C(10)-C(9)	0.7(7)	C(4)-C(29)-C(30)-C(31)	175.6(5)
P(1)-C(5)-C(10)-C(9)	-179.8(4)	C(29)-C(30)-C(31)-C(32)	0.1(8)
C(2)-C(1)-C(11)-C(12)	-21.4(6)	C(30)-C(31)-C(32)-C(33)	1.2(8)
P(1)-C(1)-C(11)-C(12)	96.8(5)	C(31)-C(32)-C(33)-C(34)	-1.3(8)
C(2)-C(1)-C(11)-C(16)	160.0(4)	C(32)-C(33)-C(34)-C(29)	0.3(8)
P(1)-C(1)-C(11)-C(16)	-81.8(5)	C(30)-C(29)-C(34)-C(33)	1.0(7)
C(16)-C(11)-C(12)-C(13)	-0.5(7)	C(4)-C(29)-C(34)-C(33)	-175.8(4)

Table S10. Atoms deviations from the plane defined by atoms C1..C4, C17 and C23 in **PPPO** (Å).

Atom	C1	C2	C3	C4	C17	C23
Deviation*	-0.0129(33)	-0.0310(47)	-0.0192(46)	0.0362(34)	0.0369(31)	-0.0100(31)

* +/- signs state for deviations in different directions.

The dihedral angles for the planes defined by atoms C1..C4, C17, C23 and Ph rings are 45.45(19)° for Ph=C17..C22, 45.41(17)° for Ph=C23..C28.

Noncovalent packing effects do not seem to influence the structures – only a few negligible intermolecular interactions are observed: C-HPh··H-CPh, C-HPh··CPh, C-HPh··O for H_2PPPO/H_2PPPO, and C4-H4··O for H_2PPPO. Therefore, the structures H_2PPPO and H_2PPPO are nearly unperturbed by the intermolecular interactions in the crystalline state.

Theoretical Calculations

Geometry optimization for PPP, PPPO and H_2PPPO and vibrational frequency calculations were performed using the B3LYP[8,9,10] hybrid functional and 6-31+G(d)[11,12,13,14,15] basis set, the D3 version of Grimme's dispersion with Becke-Johnson damping (GD3BJ)[16,17] and the polarizable continuum model of MeCN in Gaussian16[18]. For all optimized structures, all frequencies of the vibrational spectrum were positive.

The calculated absorption and emission peaks of PPP, PPPO and H_2PPPO by means of the time-dependent density functional theory (TDDFT) method and the ωB97X-D [19] /def2SVP [20] scrf=(solvent=acetonitrile,pcm) [21 , 22] level agree well with the experimental results. Natural-transition-orbital (NTO)[23] calculations were performed for the first three transitions.

To analyze the degree of aromaticity of the five-membered P-heterocycles of the phosphole, H_2PPPO, PPPO and PPP molecules, the HOMA (Harmonic Oscillator Model of Aromaticity)[24,25] values were calculated using the MultiWFN software package [26]. Preliminarily the molecular structure of all compounds was optimized by the B3LYP method in combination with the 6-31+G(d) basis set. Since the H_2PPPO, PPPO, and PPP molecules contain a large number of phenyl groups actively participating in the stacking interaction, the empirical D3BJ corrections were used to more accurately describe the dispersion interaction. The effect of the solvent on the molecular structure of the compounds was taken into account using the PCM continuum model (solvent - acetonitrile).

Another parameter used in this work to quantify aromaticity is NICS(0) (Nucleus-Independent Chemical Shifts)[27] which characterizes the degree of shielding at a point located within the five-membered cycle. As such a point, we chose a cyclic critical point of the type (3; +1), localized as a result of the analysis of the topology of the total electron density in the framework of the quantum theory of atoms in molecules (QTAIM)[28]. QTAIM analysis was performed by AIMAll software[29]. The calculation of the NICS(0) values was performed for the optimized structures in the same B3LYP/6-31+G(d) D3BJ level of theory that was used to calculate the HOMA values.

1,2,3,4,5-pentaphenylphosphole (PPP)

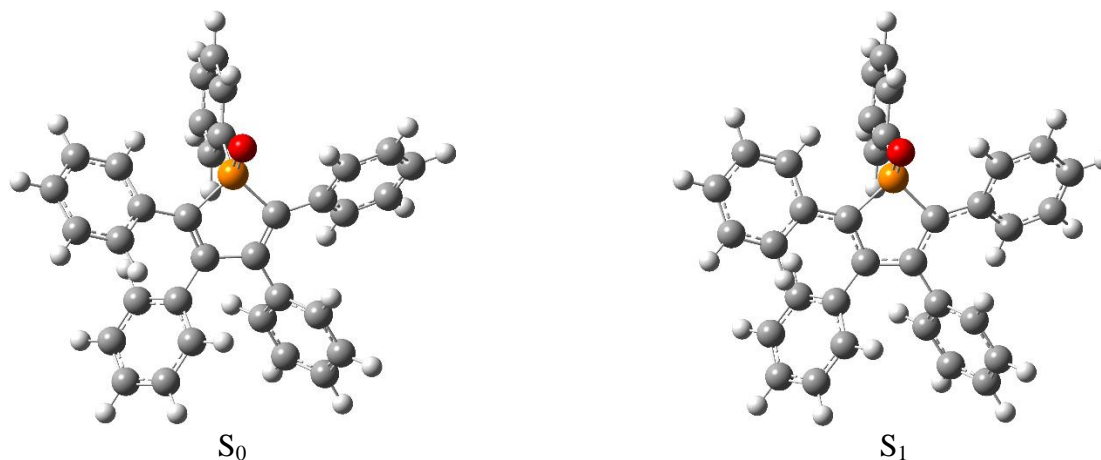S_0 S_1
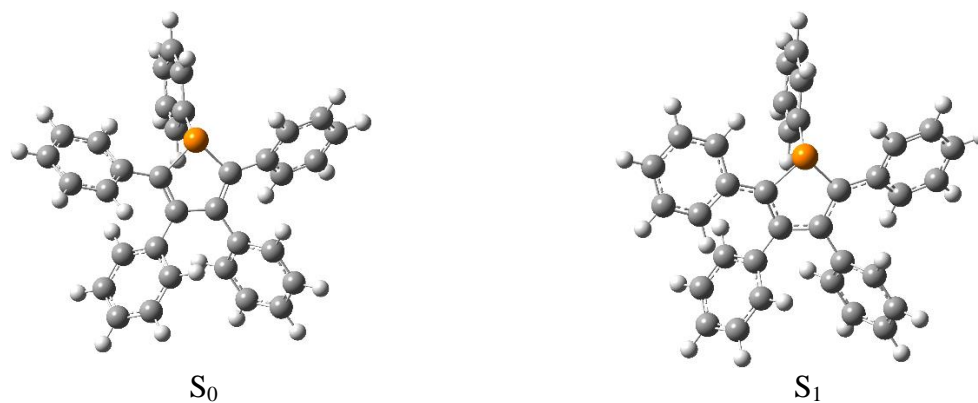
Figure S9. Optimized geometry of PPP S_0 and S_1.

Table S11. Oscillator strength of PPP.

Excitation. UV-Vis spectrum, λ (oscillator strength)		**Emission.** UV-Vis spectrum, λ (oscillator strength)		**Experiment**
	3) 255 nm (0.23) 2) 277 nm (0.31) 1) 330 nm (0.25)		3) 304 nm (0.42) 2) 328 nm (0.28) 1) 513 nm (0.53)	Absorption: 217 nm, 257 nm, 360 nm Emission: 473 nm
Excited State 1:	**330.00 nm f=0.2490** 122 ->123 0.68379	Excited State 1:	**512.80 nm f=0.5337** 122 ->123 0.69666	
Excited State 2:	**277.23 nm f=0.3137** 112 ->123 0.10275 119 ->123 -0.20863 120 ->123 -0.22180 121 ->123 0.59336	Excited State 2:	**328.03 nm f=0.2803** 112 ->123 0.14145 114 ->123 -0.10049 120 ->123 -0.40468 121 ->123 0.50491	
Excited State 3:	**254.71 nm f=0.2259** 119 ->123 0.14195	Excited State 3:	**304.21 nm f=0.4160** 120 ->123 0.42136	

	120 ->123 0.44202			121 ->123 0.41898	
	121 ->123 0.26588			122 ->124 0.28603	
	122 ->124 0.30335			122 ->125 0.16412	
	122 ->125 0.22919				
	122 ->127 0.10115				

NTO analysis
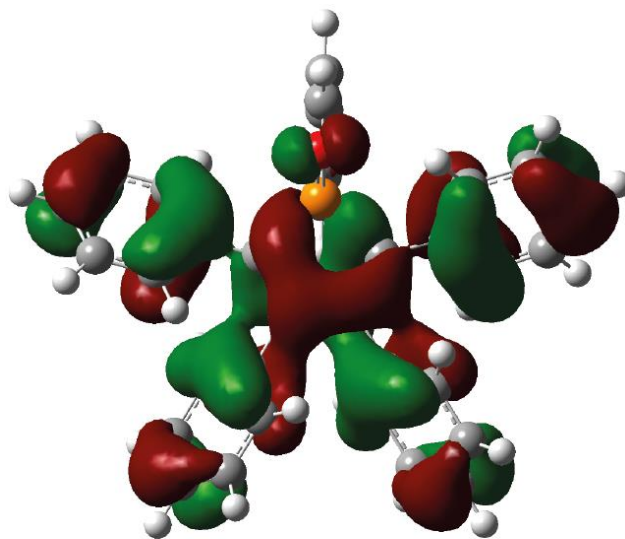
for optimized geometry of PPP:

1) # td wb97xd scrf=(solvent=acetonitrile,pcm) def2svp
2) # wb97xd scrf=(solvent=acetonitrile,pcm) Geom=AllCheck Pop=(Minimal,NTO,saveNTO) def2svp Guess=(Read,Only)
   Density=(Check,Transition=1)
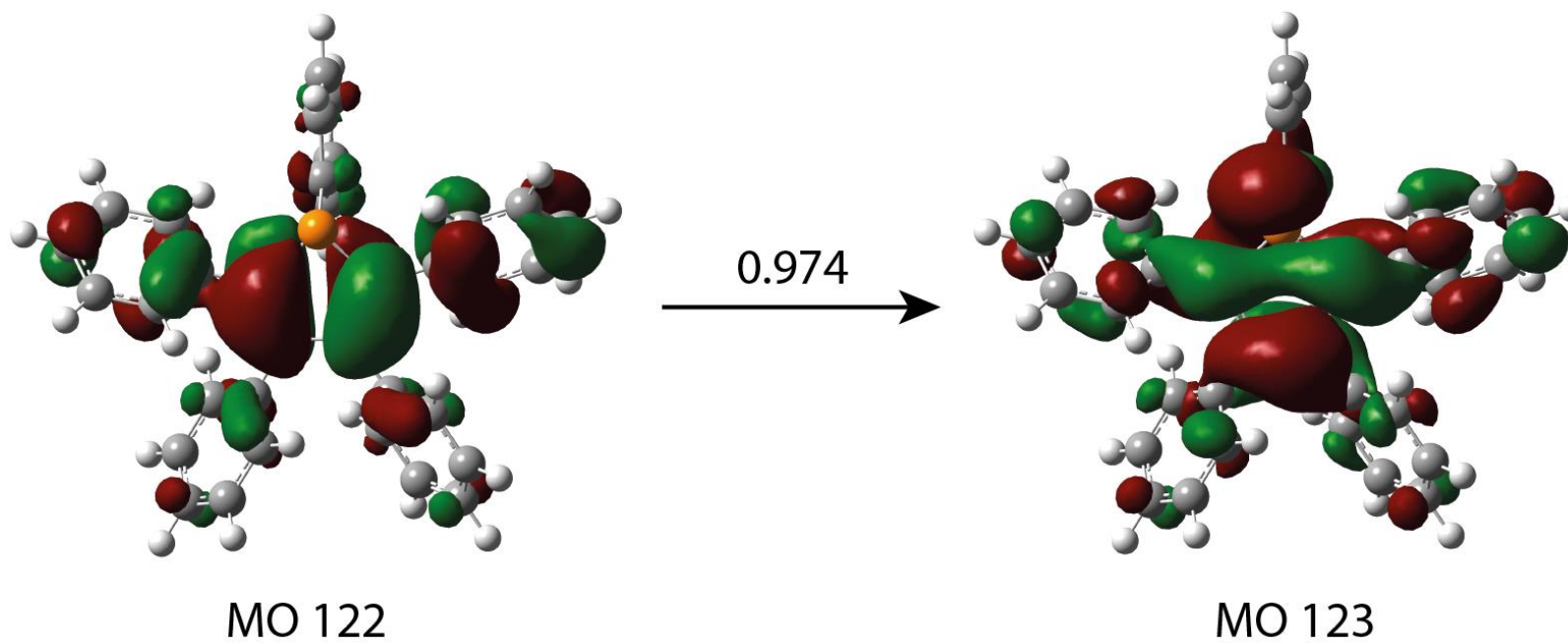
Figure S10. Molecular orbitals of PPP.

for optimized geometry of PPP:

1) # td wb97xd scrf=(solvent=acetonitrile,pcm) def2svp
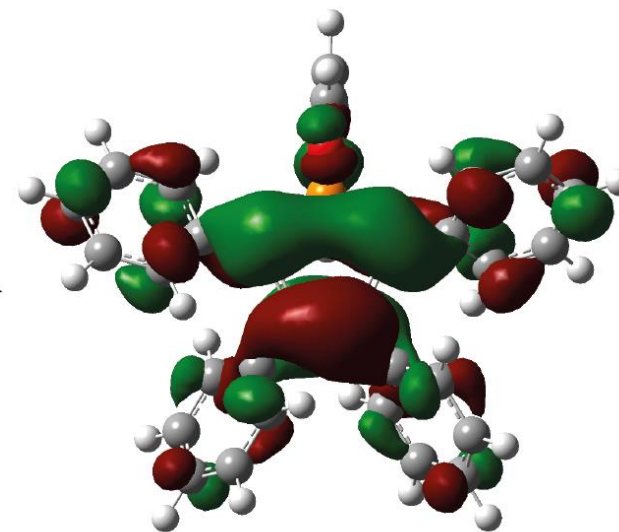2) # wb97xd scrf=(solvent=acetonitrile,pcm) Geom=AllCheck Pop=(Minimal,NTO,saveNTO) def2svp Guess=(Read,Only) **Density=(Check,Transition=2)**
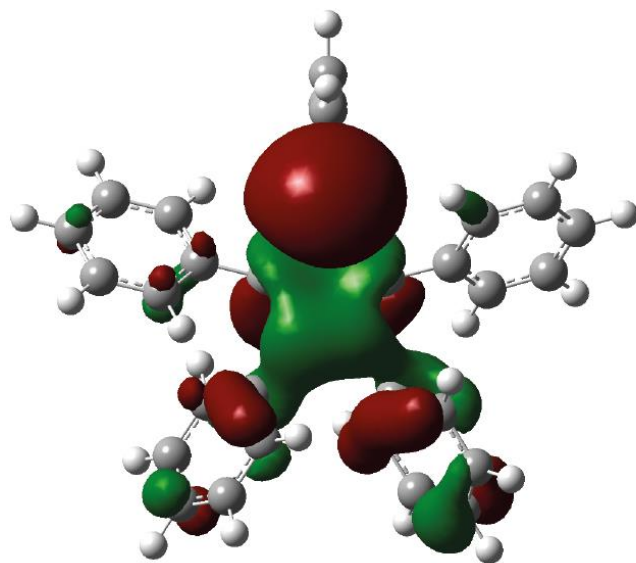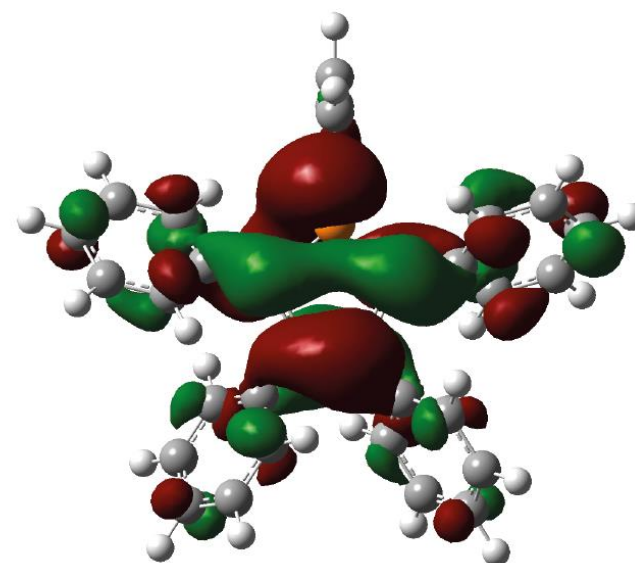
Figure S11. Molecular orbitals of PPP.

for optimized geometry of PPP:

1) # td wb97xd scrf=(solvent=acetonitrile,pcm) def2svp
2) # wb97xd scrf=(solvent=acetonitrile,pcm) Geom=AllCheck Pop=(Minimal,NTO,saveNTO) def2svp Guess=(Read,Only) **Density=(Check,Transition=3)**

MO 122

0.623 →

MO 123

MO 121

0.331 →

MO 124
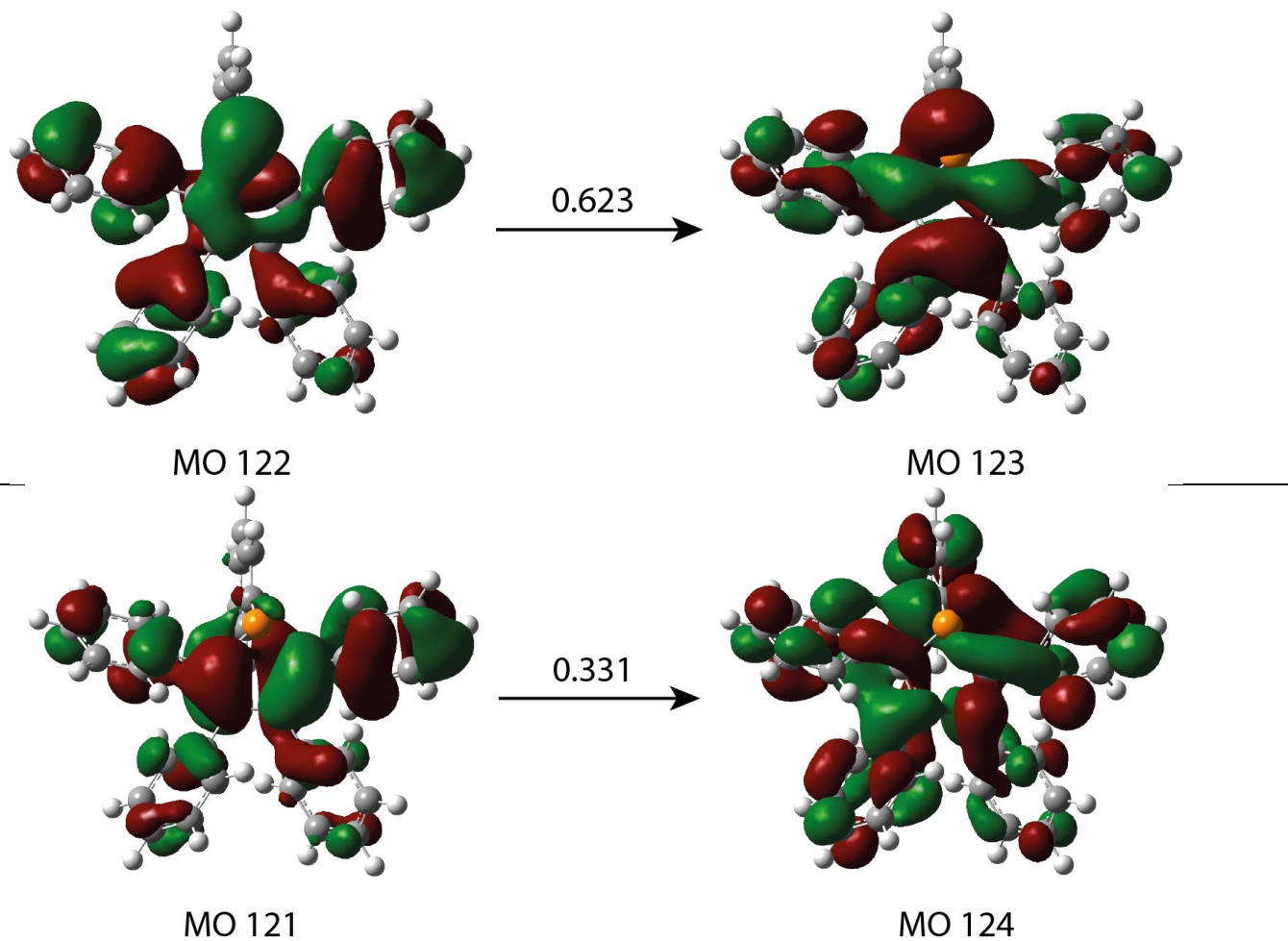
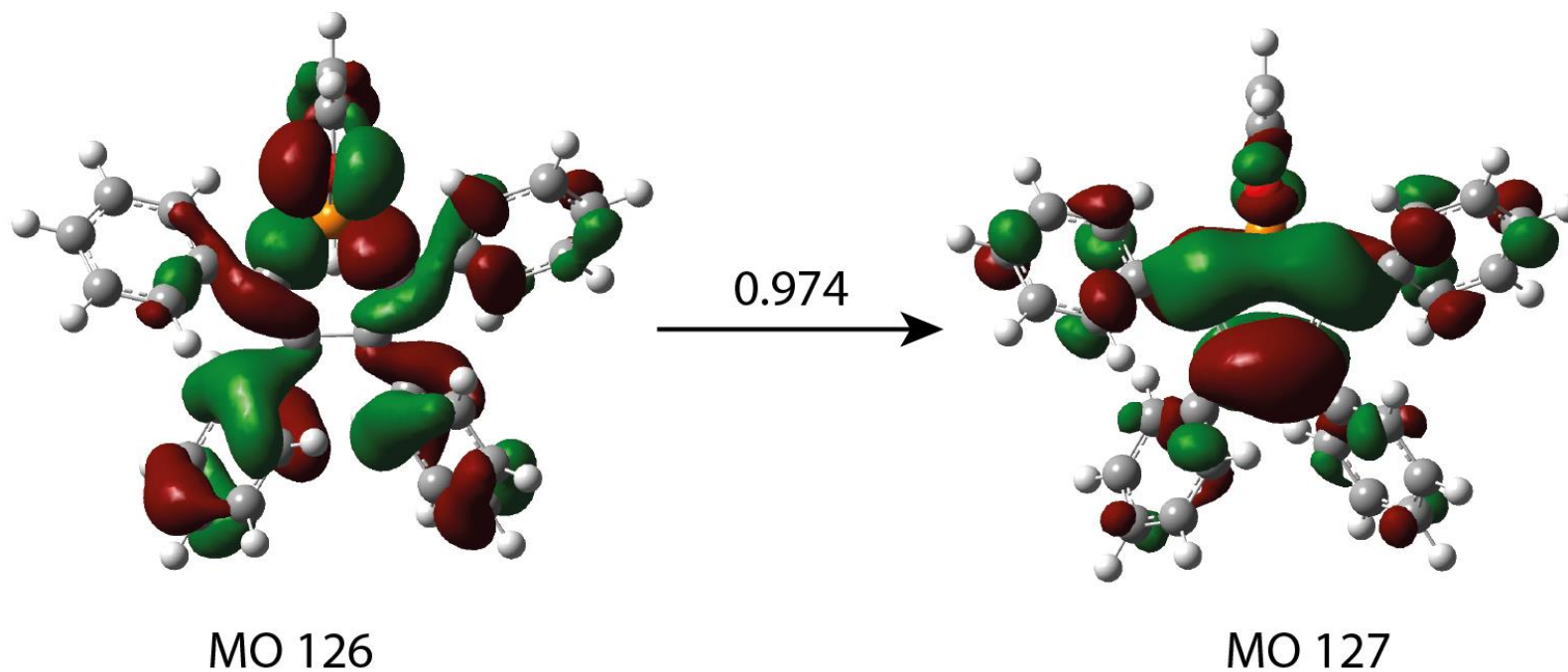Figure S12. Molecular orbitals of PPP.

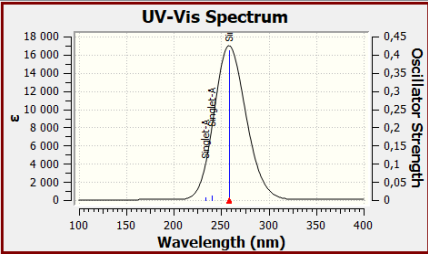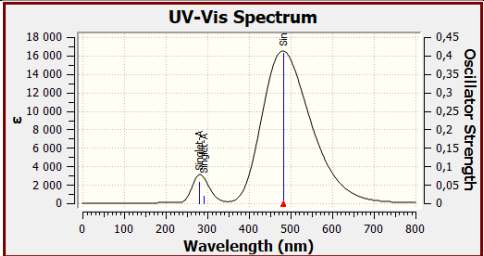**1,2,3,4,5-pentaphenylphospholoxide (PPPO)**

S₀ — S₁

Figure S13. Optimized geometry of PPPO S_0 and S_1.

Table S12. Oscillator strength of PPPO.

Excitation. UV-Vis spectrum, λ (oscillator strength)		Emission. UV-Vis spectrum, λ (oscillator strength)		Experiment
	3) 279 nm (0.07) 2) 283 nm (0.29) 1) 368 nm (0.23)		3) 326 nm (0.03) 2) 342 nm (0.45) 1) 588 nm (0.39)	Absorption: 205 nm, 257 nm, 380 nm Emission: 539 nm
Excited State 1:	**367.50 nm f=0.2267** 126 ->127 0.68372	Excited State 1:	**587.52 nm f=0.3878** 126 ->127 -0.69648	
Excited State 2:	**282.83 nm f=0.2887** 124 ->127 -0.18105 125 ->127 0.63707	Excited State 2:	**342.39 nm f=0.4526** 125 ->127 0.68359	
Excited State 3:	**279.09 nm f=0.0745** 114 ->127 -0.10673	Excited State 3:	**326.36 nm f=0.0282** 115 ->127 -0.28683	

115 ->127	-0.20874		119 ->127	-0.32418
120 ->127	-0.23255		121 ->127	-0.12111
122 ->127	-0.21724		122 ->127	0.38558
124 ->127	0.48302		124 ->127	0.31186
125 ->127	0.23151			

NTO analysis

for the optimized geometry of PPPO:

1) # td wb97xd scrf=(solvent=acetonitrile,pcm) def2svp
2) # wb97xd scrf=(solvent=acetonitrile,pcm) Geom=AllCheck Pop=(Minimal,NTO,saveNTO) def2svp Guess=(Read,Only)
   Density=(Check,Transition=1)
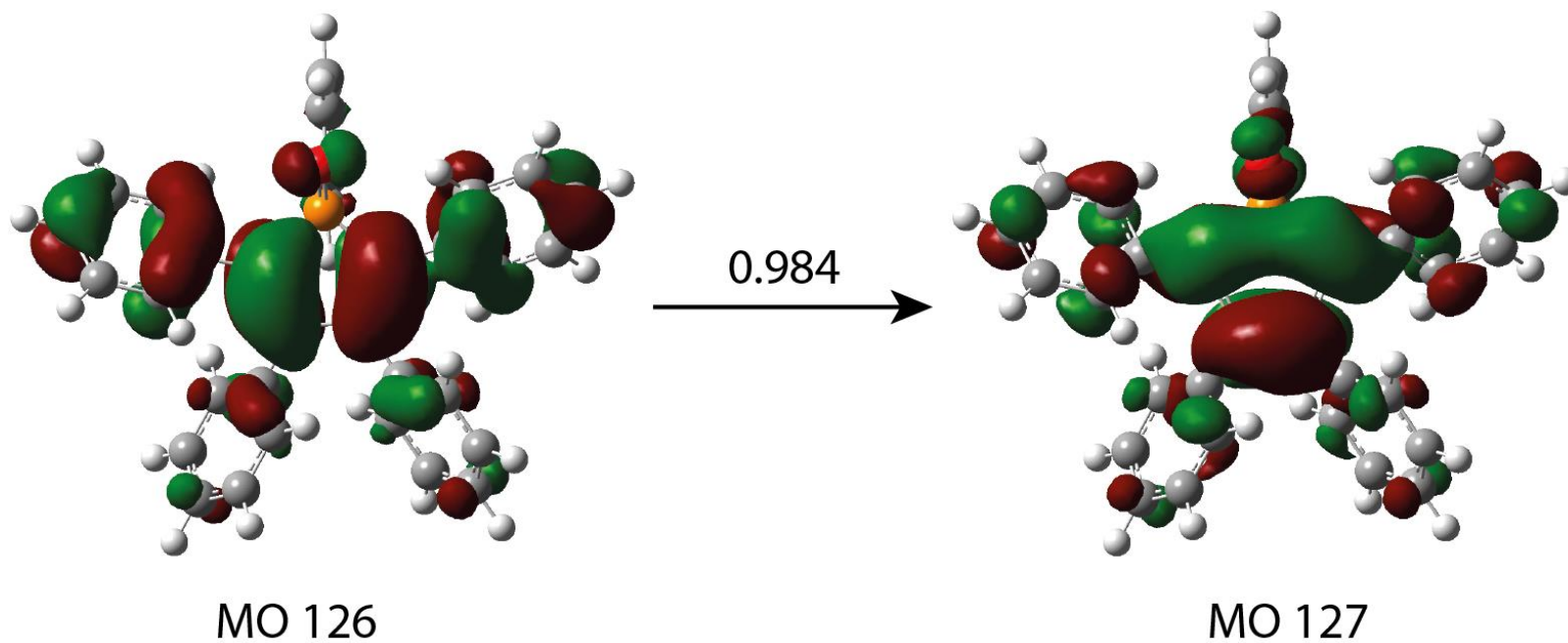
Figure S14. Molecular orbitals of PPPO.

for the optimized geometry of PPPO:

1) # td wb97xd scrf=(solvent=acetonitrile,pcm) def2svp
2) # wb97xd scrf=(solvent=acetonitrile,pcm) Geom=AllCheck Pop=(Minimal,NTO,saveNTO) def2svp Guess=(Read,Only) **Density=(Check,Transition=2)**
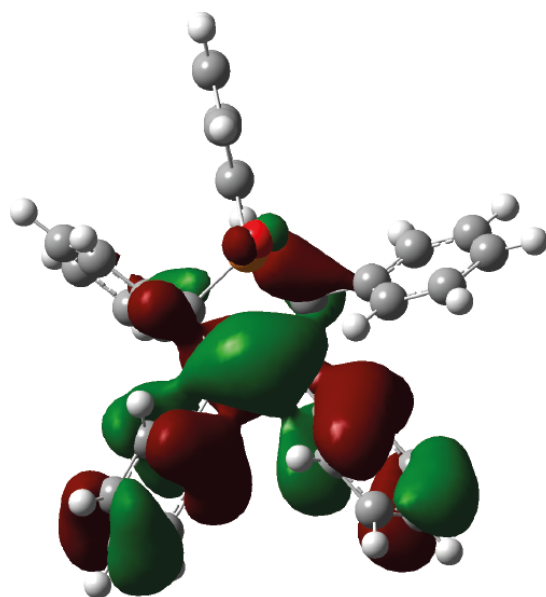

Figure S15. Molecular orbitals of PPPO.

for the optimized geometry of PPPO:

1) # td wb97xd scrf=(solvent=acetonitrile,pcm) def2svp
2) # wb97xd scrf=(solvent=acetonitrile,pcm) Geom=AllCheck Pop=(Minimal,NTO,saveNTO) def2svp Guess=(Read,Only) **Density=(Check,Transition=3)**


131	0.00137
130	0.00261
129	0.00515
128	0.01453
127	0.97374
126	0.97374
125	0.01453
124	0.00515
123	0.00261
122	0.00137

MO 126

0.974

MO 127

Figure S16. Molecular orbitals of PPPO.

1,2,3,4,5-pentaphenyl-2,5-dihydrophosphole-1-oxide (H₂PPPO)

S₀   S₁
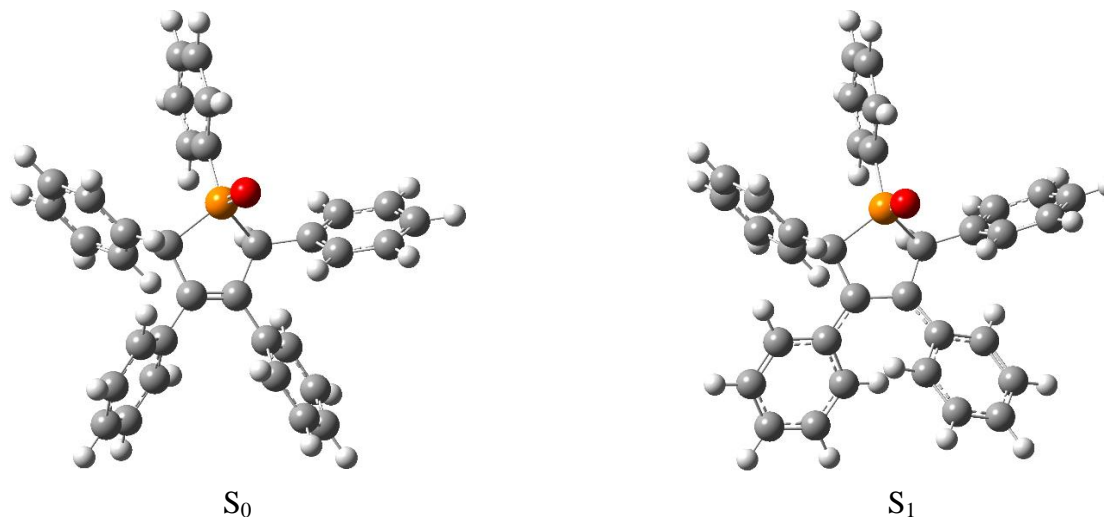
Figure S17. Optimized geometry of H₂PPPO S₀ and S₁.

Table S13. Oscillator strength of H₂PPPO.

| **Excitation.** UV-Vis spectrum, λ (oscillator strength)		**Emission.** UV-Vis spectrum, λ (oscillator strength)		**Experiment**
	3) 234 nm (0.01) 2) 240 nm (0.01) 1) 258 nm (0.41)		3) 279 nm (0.06) 2) 291 nm (0.02) 1) 481 nm (0.41)	Absorption: 225 nm, 257 nm Emission: 429 nm
Excited State 1:	**258.46 nm f=0.4115** 127 ->128 0.64650 127 ->129 -0.20960	Excited State 1:	**481.15 nm f=0.4067** 127 ->128 0.70127	
Excited State 2:	**239.51 nm f=0.0125** 121 ->133 0.13167 121 ->136 0.12634	Excited State 2:	**291.43 nm f=0.0212** 122 ->128 -0.12802 123 ->128 -0.14661	

	122 ->128 0.14772 123 ->128 0.15856 124 ->128 0.26491 124 ->129 -0.11284 127 ->130 0.33873 127 ->131 -0.10945 127 ->134 0.20655 127 ->135 0.14080		124 ->128 0.44475 125 ->128 0.19098 126 ->128 -0.19351 127 ->130 -0.28241 127 ->131 0.18143 127 ->132 -0.10199 127 ->135 -0.14062	
Excited State 3:	**233.69 nm f=0.0075** 118 ->128 -0.15291 119 ->128 0.13546 121 ->128 0.25817 121 ->130 0.11822 121 ->134 0.11154 122 ->134 0.10192 124 ->136 0.11603 126 ->128 0.14145 127 ->132 -0.10099 127 ->133 0.21767 127 ->135 0.14593 127 ->136 0.10948 127 ->137 0.20497	Excited State 3:	**279.27 nm f=0.0579** 124 ->128 0.17295 126 ->128 0.63328	

NTO analysis

for the optimized geometry of H₂PPPO:

1) # td wb97xd scrf=(solvent=acetonitrile,pcm) def2svp
2) # wb97xd scrf=(solvent=acetonitrile,pcm) Geom=AllCheck Pop=(Minimal,NTO,saveNTO) def2svp Guess=(Read,Only)
   **Density=(Check,Transition=1)**
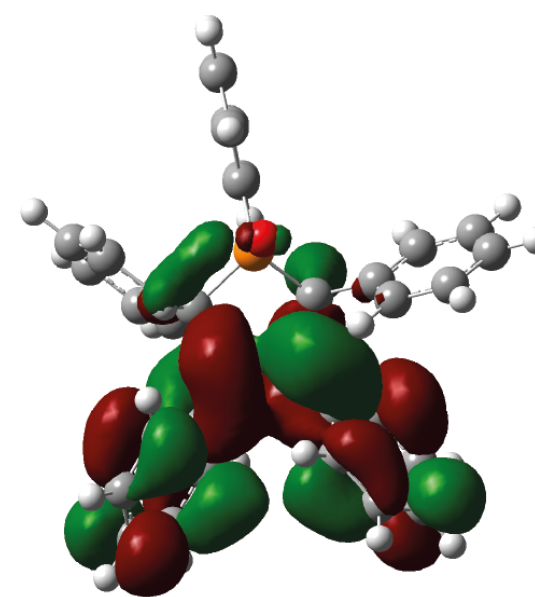
Figure S18. Molecular orbitals of H₂PPPO.

for the optimized geometry of H₂PPPO:

1) # td wb97xd scrf=(solvent=acetonitrile,pcm) def2svp
2) # wb97xd scrf=(solvent=acetonitrile,pcm) Geom=AllCheck Pop=(Minimal,NTO,saveNTO) def2svp Guess=(Read,Only) **Density=(Check,Transition=2)**
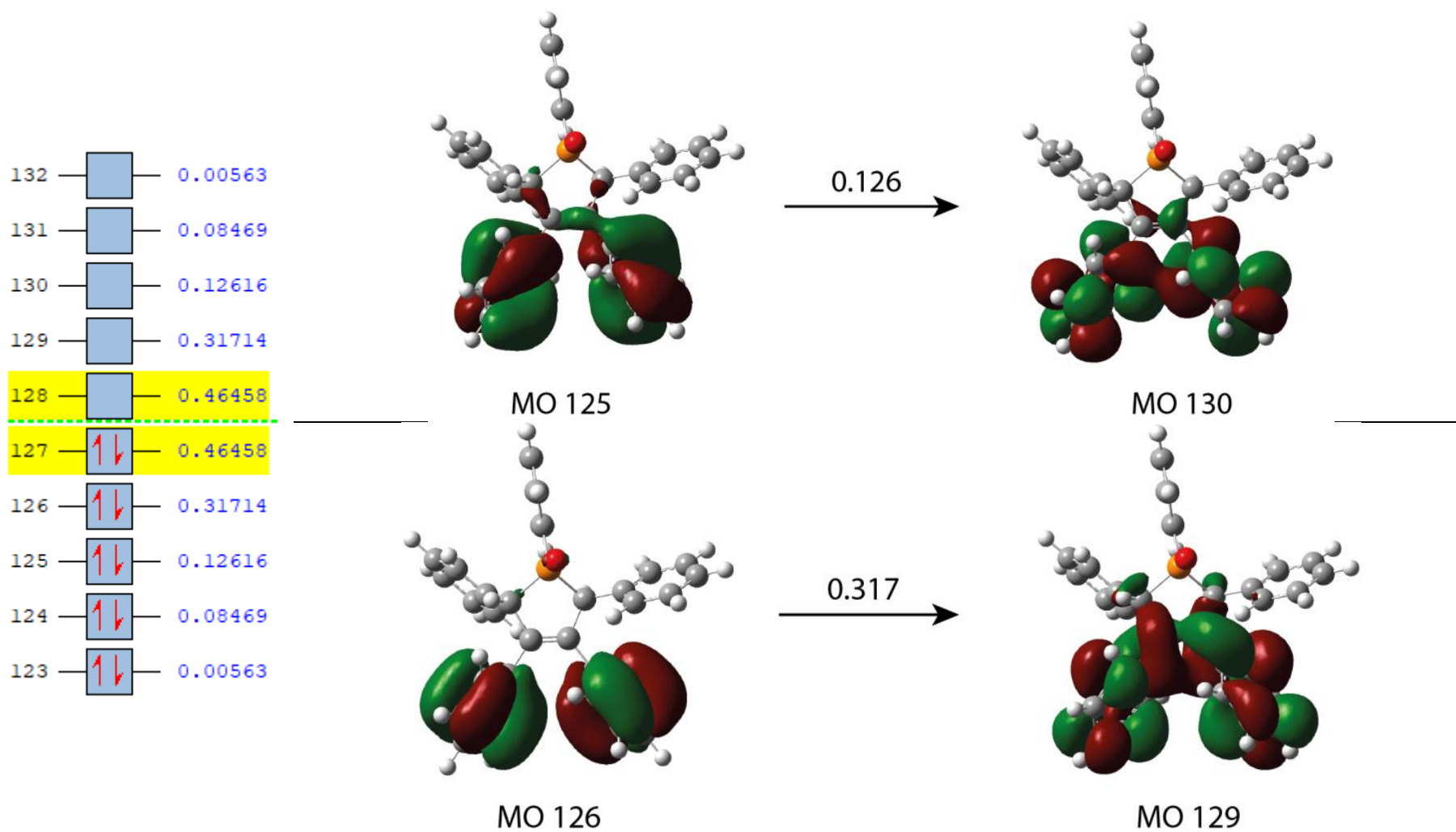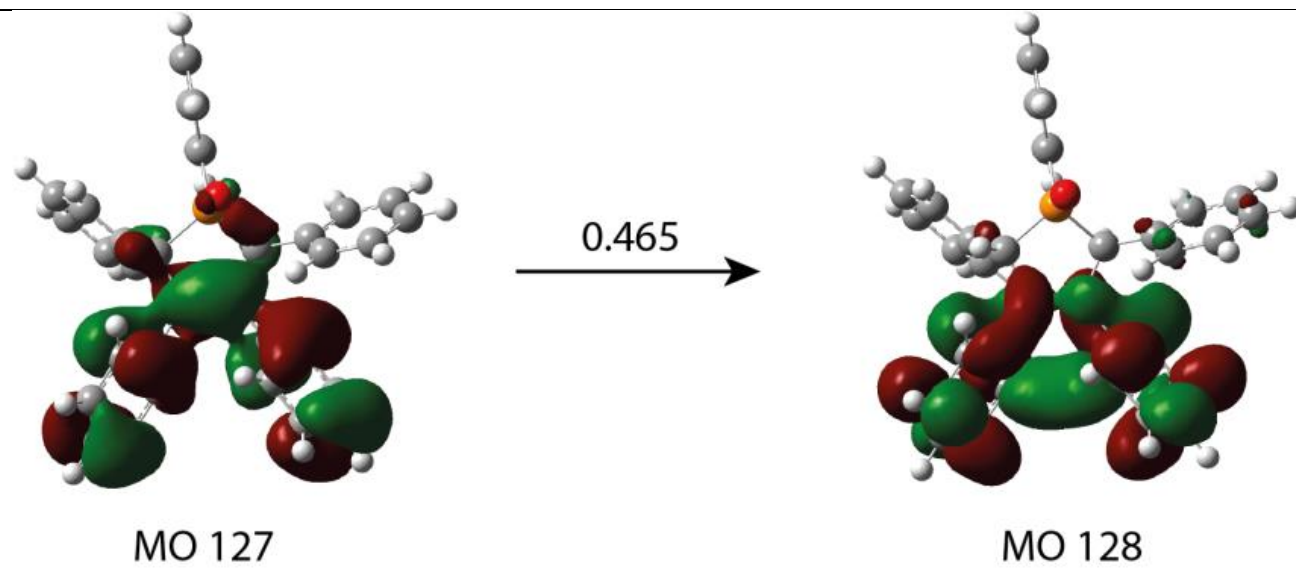
Figure S19. Molecular orbitals of H$_2$PPPO.

for the optimized geometry of H₂PPPO:

1) # td wb97xd scrf=(solvent=acetonitrile,pcm) def2svp

2) # wb97xd scrf=(solvent=acetonitrile,pcm) Geom=AllCheck Pop=(Minimal,NTO,saveNTO) def2svp Guess=(Read,Only)
   Density=(Check,Transition=3)
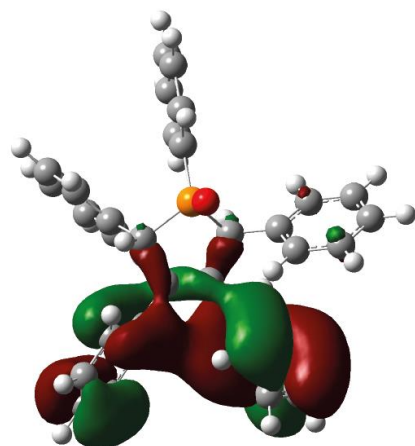
MO 124 → 0.140 → MO 131

MO 125 → 0.154 → MO 130

MO 126   0.304   MO 129

MO 127   0.364   MO 128
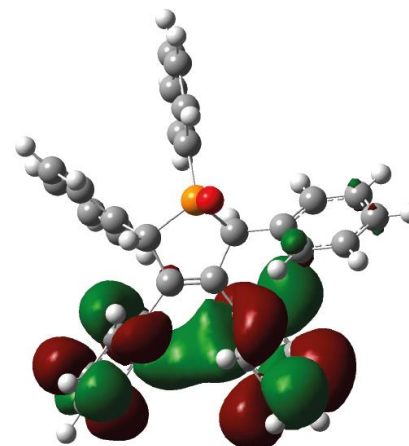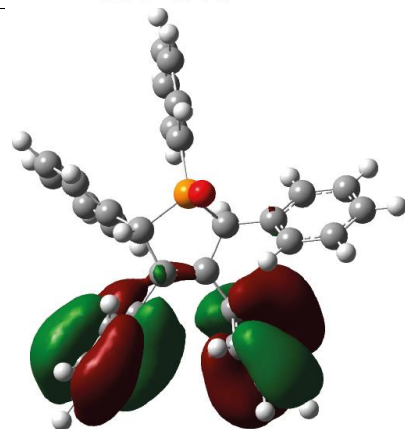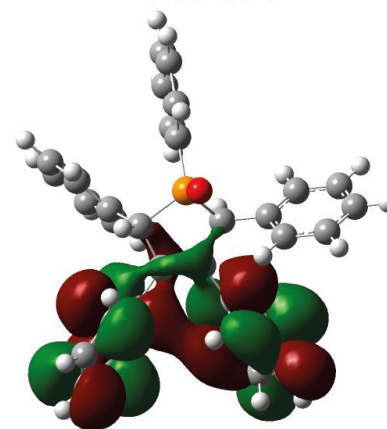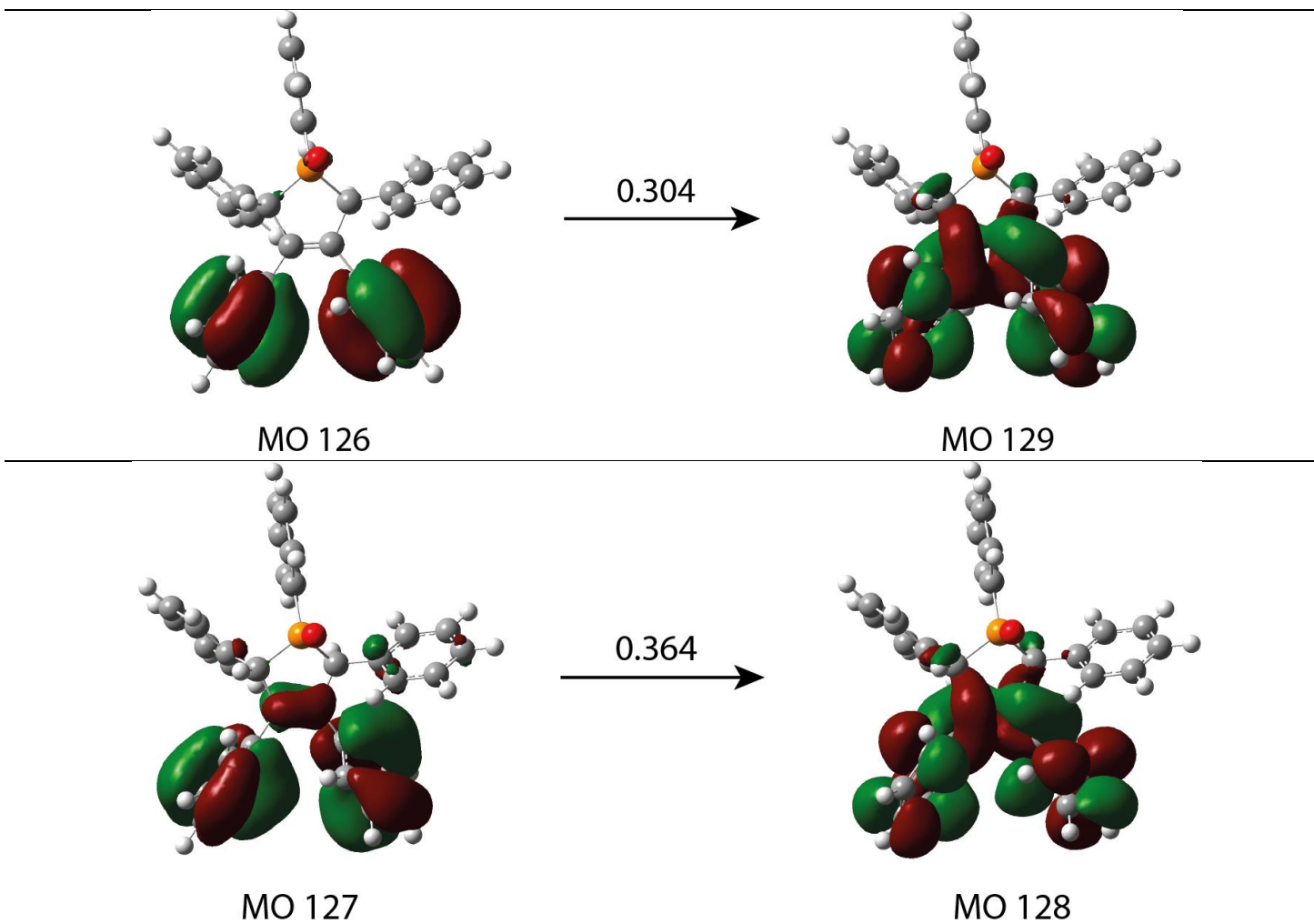
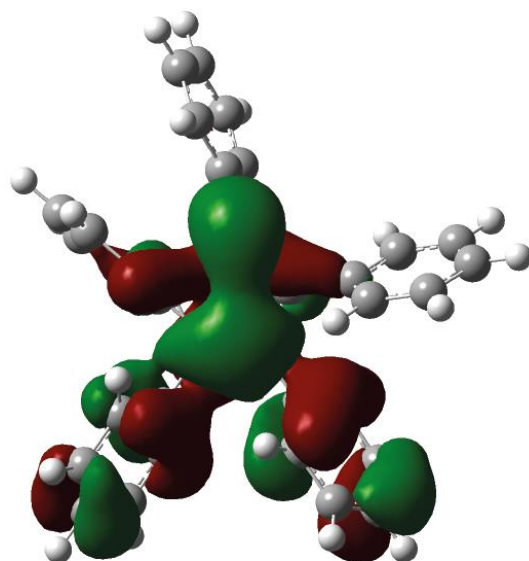Figure S20. Molecular orbitals of H$_2$PPPO.

1,2,3,4,5-pentaphenyl-2,5-dihydrophosphole (H₂PPP)

S₀   S₁
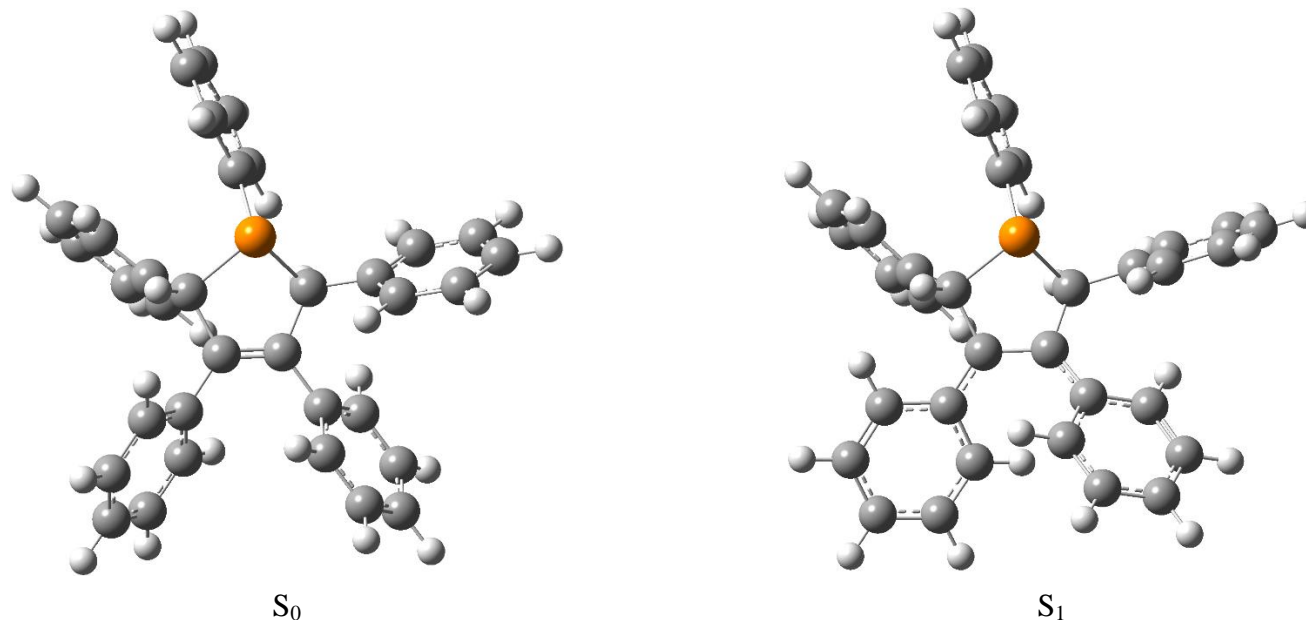
Figure S21. Optimized geometry of H₂PPP S₀ and S₁.

Table S14. Oscillator strength of H₂PPP.

Excitation. UV-Vis spectrum, λ (oscillator strength)		**Emission.** UV-Vis spectrum, λ (oscillator strength)	
	3) 293 nm (0.02) 2) 246 nm (0.20) 1) 260 nm (0.26)		3) 290 nm (0.01) 2) 300 nm (0.01) 1) 484 nm (0.40)
Excited State 1:	**260.42 nm f=0.2596**	Excited State 1:	**484.43 nm f=0.3995**

	122 ->124 -0.11483 122 ->125 -0.11089 123 ->124 0.65172		123 ->124 0.70133
Excited State 2:	**246.47 nm f=0.1957** 121 ->124 -0.13979 122 ->124 0.52072 122 ->125 0.29385 123 ->124 0.14940 123 ->125 -0.14199	Excited State 2:	**300.26 nm f=0.0030** 115 ->124 0.10152 121 ->124 -0.17201 122 ->124 0.63942
Excited State 3:	**239.03 nm f=0.0169** 114 ->133 0.13038 116 ->130 -0.14077 117 ->124 0.13098 118 ->124 -0.27113 119 ->124 0.11717 123 ->125 0.10108 123 ->126 0.33906 123 ->129 0.20627 123 ->130 0.14452 123 ->132 0.10853	Excited State 3:	**289.68 nm f=0.0044** 117 ->124 0.15607 119 ->124 0.44891 121 ->124 -0.18433 123 ->125 -0.10337 123 ->126 -0.34940 123 ->129 0.19244

NTO analysis

for the optimized geometry of H$_2$PPP:

1) # td wb97xd scrf=(solvent=acetonitrile,pcm) def2svp
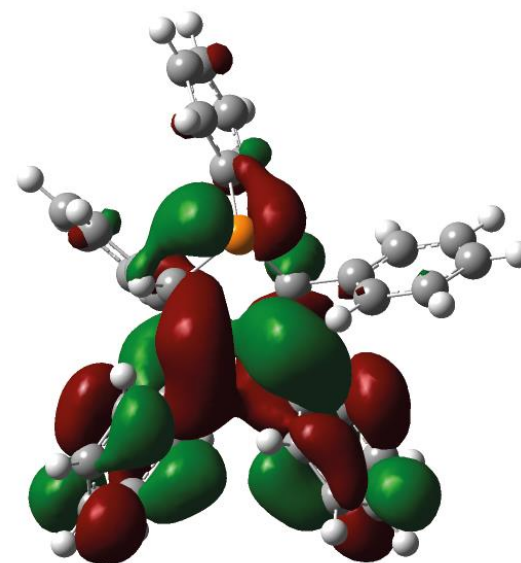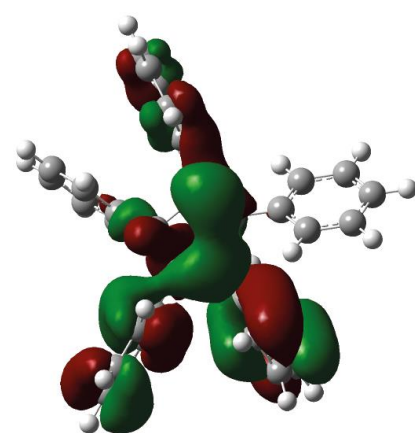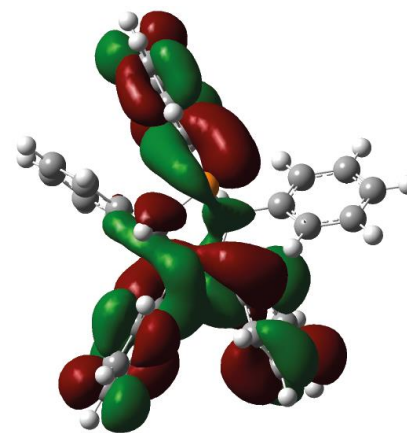2) # wb97xd scrf=(solvent=acetonitrile,pcm) Geom=AllCheck Pop=(Minimal,NTO,saveNTO) def2svp Guess=(Read,Only) **Density=(Check,Transition=1)**

Figure S22. Molecular orbitals of H$_2$PPP.

for the optimized geometry of H$_2$PPP:

1) # td wb97xd scrf=(solvent=acetonitrile,pcm) def2svp
2) # wb97xd scrf=(solvent=acetonitrile,pcm) Geom=AllCheck Pop=(Minimal,NTO,saveNTO) def2svp Guess=(Read,Only)
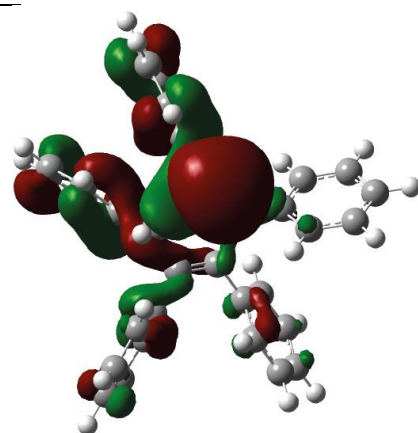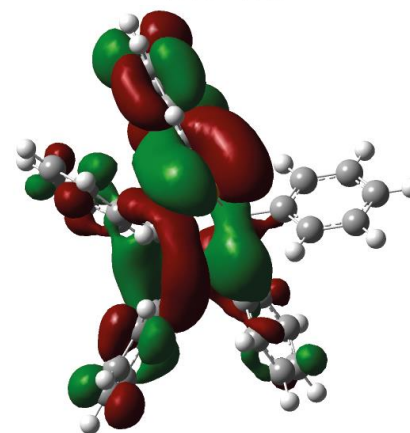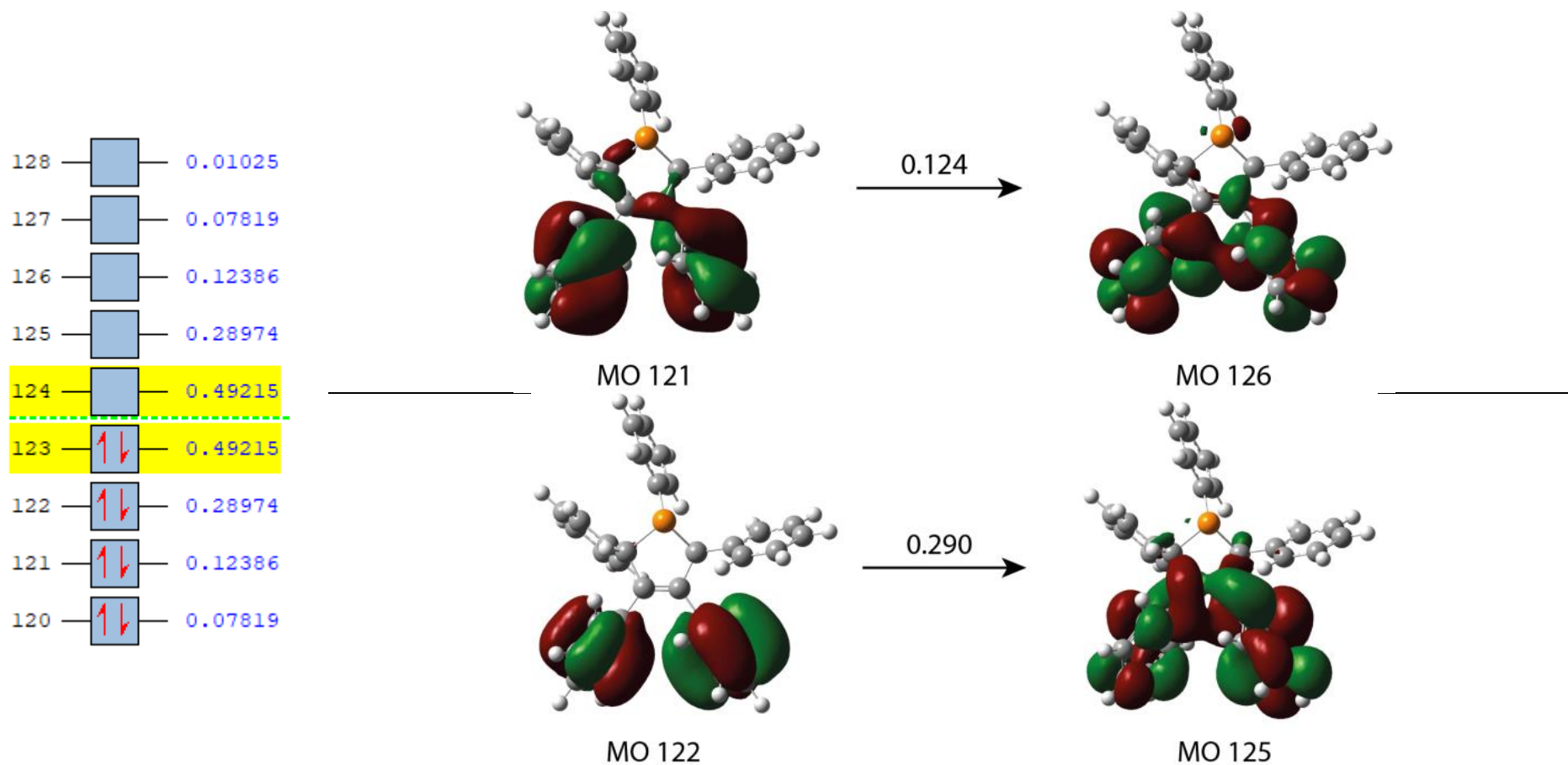   **Density=(Check,Transition=2)**

MO 122

MO 125

MO 123

MO 124

Figure S23. Molecular orbitals of H$_2$PPP.

for the optimized geometry of H₂PPP:

1) # td wb97xd scrf=(solvent=acetonitrile,pcm) def2svp
2) # wb97xd scrf=(solvent=acetonitrile,pcm) Geom=AllCheck Pop=(Minimal,NTO,saveNTO) def2svp Guess=(Read,Only)
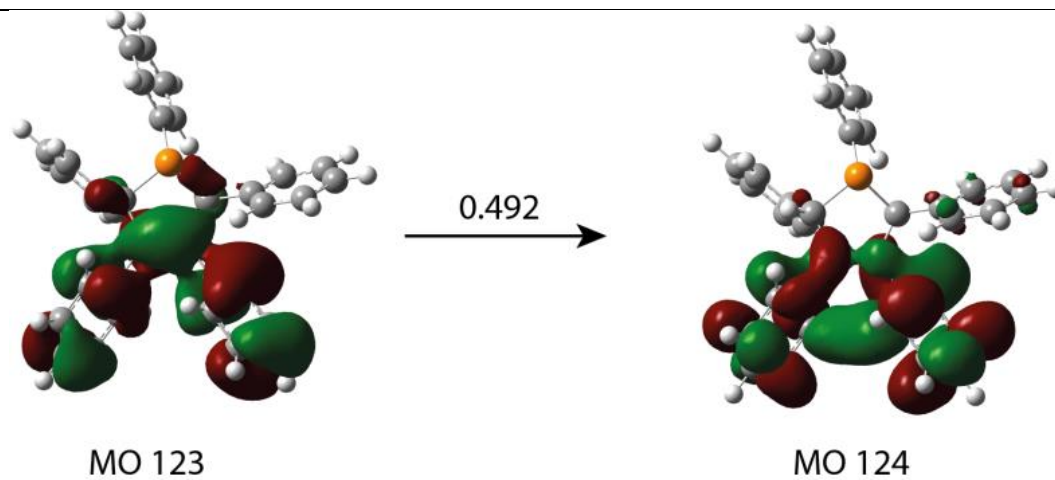   **Density=(Check,Transition=3)**

MO 123   0.492   MO 124

Figure S24. Molecular orbitals of H_2PPP.

Literature references:

[1] A. S. Galushko, E. G. Gordeev and V. P. Ananikov, *Langmuir*, 2018, **34**, 15739-15748.

[2] B. Z. Tang, X. Zhan, G. Yu, P. P. Sze Lee, Y. Liu and D. Zhu, *J. Mater. Chem.*, 2001, **11**, 2974-2978.

[3] J.-C. G. Bünzli, S.V. Eliseeva, Lanthanide Luminescence, *Springer Series on Fluorescence,* 2010, **7**, 1-45.

[4] Bruker. *Bruker AXS Inc.*, Madison, Wisconsin, USA, 2021.

[5] L. Krause, R. Herbst-Irmer, G. M. Sheldrick, D. Stalke, *J. Appl. Crystallogr.,* 2015, **48**, 3-10.

[6] G. M. Sheldrick, *Acta Crystallogr., Sect. A,* 2015, **71**, 3-8.

[7] G. M. Sheldrick, *Acta Crystallogr., Sect. C,* 2015, **71**, 3-8.

[8] A. D. Becke, *Phys. Rev. A*, 1988, **38**, 3098.

[9] C. Lee, W. Yang, and R. G. Parr, *Phys. Rev. B,* 1988*,* **37**, 785.

[10] A. D. Becke , *J. Chem. Phys.*, 1993, **98**, 5648.

[11] M. M. Francl, W. J. Pietro, W. J. Hehre, *J. Chem. Phys.*, 1982, **77**, 3654.

[12] W. J. Hehre, R. Ditchfield, and J. A. Pople, *J. Chem. Phys.*, 1972, **56**, 2257.

[13] A. D. McLean, *J. Chem. Phys.,* 1980, **72**, 5639.

[14] R. Krishnan, J. S. Binkley, R. Seeger, J. A. Pople, *J. Chem. Phys.,* 1980*,* **72**, 650.

[15] I. V. Malyar, E. Titov, N. Lomadze, P. Saalfrank, S. Santer, *J. Chem. Phys.,* 2017*,* **146**, 104703.

[16] S. Grimme, J. Antony, S. Ehrlich, H. Krieg, *J. Chem. Phys., 2010,* **132**, 154104.

[17] H. Kruse, S. Grimme, *J. Chem. Phys.,* 2012*,* **136**, 154101.

[18] M. J. Frisch, G. W. Trucks, H. B. Schlegel, G. E. Scuseria, M. A. Robb, J. R. Cheeseman, G. Scalmani, V. Barone, G. A. Petersson, H. Nakatsuji, X. Li, M. Caricato, A. V. Marenich, J. Bloino, B. G. Janesko, R. Gomperts, B. Mennucci, H. P. Hratchian, J. V. Ortiz, A. F. Izmaylov, J. L. Sonnenberg, D. F. Williams-Young, Ding, F. Lipparini, F. Egidi, J. Goings, B. Peng, A. Petrone, T. Henderson, D. Ranasinghe, V. G. Zakrzewski, J. Gao, N. Rega, G. Zheng, W. Liang, M. Hada, M. Ehara, K. Toyota, R. Fukuda, J. Hasegawa, M. Ishida, T. Nakajima, Y. Honda, O. Kitao, H. Nakai, T. Vreven, K. Throssell, J. A., Jr. Montgomery, J. E. Peralta, F. Ogliaro, M. J. Bearpark, J. J. Heyd, E. N. Brothers, K. N. Kudin, V. N. Staroverov, T. A. Keith, R. Kobayashi, J. Normand, K. Raghavachari, A. P. Rendell, J. C. Burant, S. S. Iyengar, J. Tomasi, M. Cossi, J. M. Millam, M. Klene, C. Adamo, R. Cammi, J. W. Ochterski, R. L. Martin, K. Morokuma, O. Farkas, J. B. Foresman, D. J. Fox, Gaussian 16 Revision C.01, Inc., Wallingford CT, 2016.

[19] Chai, J.-D.; Head-Gordon, M. *Phys. Chem. Chem. Phys.* 2008, **10**, 6615−6620.

[20] Weigend, F.; Ahlrichs, R. *Phys. Chem. Chem. Phys.* 2005, **7**, 3297–3305.

[21] J. Ingenmey, M. von Domaros, E. Perlt, S. P. Verevkin, B. Kirchner, *J. Chem. Phys.*, 2018, **148**, 193822.

[22] B. Thomsen, M. Shiga, *J. Chem. Phys.,* 2021, **154**, 084117.

[23] R. L. Martin, *J. Chem. Phys.,* 2003, **118**, 4775-4777.

[24] J. Kruszewski and T.M. Krygowski, *Tetrahedron Lett.*, 1972, **13**, 3839-3842.

[25] T.M. Krygowski, *J. Chem. Inf. Comput. Sci.*, 1993, **33**, 70–78.

[26] T. Lu and F. Chen, *J. Comput. Chem.* 2012, **33**, 580-592.

[27] P. V. R. Schleyer, C. Maerker, A. Dransfeld, H. Jiao and N. J. R. van Eikema Hommes, *J. Am. Chem. Soc.*, 1996, **118**, 6317-6318

[28] R.F.W. Bader, Atoms in Molecules: A Quantum Theory, *Oxford University Press*, Oxford, 1990.

[29] AIMAll (Version 19.10.12), T. A. Keith, TK Gristmill Software, Overland Park KS, USA, 2019 (aim.tkgristmill.com).